

RESEARCH ARTICLE

Jordanian migration and mobility in the Middle Bronze Age (ca. 2100–1550 BCE) at Pella

Chris Stantis^{1,2}  | Nina Maaranen¹  | Arwa Kharobi^{1,3}  | Geoff M. Nowell⁴  |
Colin Macpherson⁴  | Holger Schutkowski¹  | Stephen Bourke⁵

¹Faculty of Science and Technology,
Department of Archaeology and
Anthropology, Bournemouth University,
Dorset, UK

²Department of Anthropology, National
Museum of Natural History, Smithsonian
Institution, Washington, DC, USA

³Université de Bordeaux, CNRS, UMR 5199:
“PACEA - De la Préhistoire à l'Actuel: Culture,
Environnement et Anthropologie”, Pessac,
France

⁴Department of Earth Sciences, Durham
University, Durham, UK

⁵Near Eastern Archaeology Foundation,
University of Sydney, Sydney, Australia

Correspondence

Chris Stantis, Faculty of Science and
Technology, Department of Archaeology and
Anthropology, Bournemouth University, Fern
Barrow, Poole, Dorset BH12 5BB,
United Kingdom.
Email: cstantis@bournemouth.ac.uk

Funding information

H2020 European Research Council, Grant/
Award Number: 668640

Abstract

The site of Pella, located in the foothills of the east Jordan valley, was a prosperous city–state throughout the Middle Bronze Age (MBA, ca. 2000–1500 BCE). As part of a widespread trading network, Pella enjoyed extensive socio-economic relationships with Egypt, Cyprus, and the Aegean, Anatolia, and Babylonia during this period. We report isotopic analysis ($^{87}\text{Sr}/^{86}\text{Sr}$, $\delta^{18}\text{O}$, and $\delta^{13}\text{C}$) from enamel of 22 human permanent second molars of which 13 second lower molars were used for an additional biodistance analysis based on ASUDAS. The multidisciplinary approach investigates the ancestral background of MBA Pella and the degree of temporary or more permanent relocation from other settlements. Ancillary to carbonate isotope analysis for migration investigation, dietary information in the form of $\delta^{13}\text{C}_{\text{carbonate}}$ was also collected. $\delta^{13}\text{C}_{\text{carbonate}}$ values (mean $-12.3\text{‰} \pm 0.4$ SD) suggest a uniform diet reliant on C_3 cereals and legumes as crops and animal fodder, adhering to expected Bronze Age Levantine dietary norms. Two methods are used to identify non-locals. Using a biospheric baseline, three individuals with non-local $^{87}\text{Sr}/^{86}\text{Sr}$ ratios are identified. Bagplot analysis of both $^{87}\text{Sr}/^{86}\text{Sr}$ and $\delta^{18}\text{O}$ data suggests that three individuals (14%) grew up elsewhere; two individuals who were already identified as $^{87}\text{Sr}/^{86}\text{Sr}$ outliers using biospheric data and one more with outlying $\delta^{18}\text{O}$ values. All individuals identified as non-locals, using either method, are from one tomb, Tomb 62. The dental nonmetric traits indicated diverse morphology and subsequent ancestry for Tomb 62 (11/13), whereas primary burials (2/13) clustered together. The commingled condition of Tomb 62 material prevented a more exhaustive biodistance analysis, but the tentative results coincide with interpretations of the tomb. Significant movements of populations throughout the Middle Bronze Age are evidenced through funerary rituals and architecture, and this study demonstrates that Pella, thought to be peripheral, nonetheless had some permanent movement evidenced through isotopes and ancestry analysis.

KEYWORDS

dental nonmetric traits, isotopes, Levant

1 | INTRODUCTION

Trade between regions, and how it functioned, is of continuous interest in Bronze Age Levantine studies. It is generally assumed that trade functioned through networks of inter-connected settlements (Ilan, 1995). Some scholars have asserted that within the general network, particular nodal sites were more critically important to the direction and regulation of trade-flow, deeming these sites “gateway communities” (Knapp, 1993). More specific to the Middle Bronze Age (MBA, ca. 2000–1500 BCE) southern Levant, it is widely assumed that the key engine of inter-regional trade was Egypt, especially after the Thirteenth Dynasty took power when Egypt adopted a more outward-facing stance (Cohen, 2018). Maritime trade along the Levantine coast with littoral ports as the essential nodes (the “port-power” model) is the assumed modus (Stager, 2001). In the later MBA, when the Hyksos rose to power in the Nile Delta, more particular links between the central driver—the Hyksos capital of Avaris (Tell el-Dab’a)—and inland south Canaanite nodes emerged (Bietak, 1997) as documented by goods such as Tell el Yahudiyeh ware and Royal Name scarabs (Bourke et al., 2006).

The site of Pella in Jordan (modern Tabaqat FahI) is located in the foothills of the east Jordan Valley approximately at sea level (McNicoll et al., 1982, 1992; Smith, 1973). The site (Figure 1) consists of a central settlement mound of perhaps six hectares in the MBA, suggesting a

town population of perhaps 1,200 at its greatest extent, not including off-site village and farmstead dwellings which may double that estimate. Blessed with a perennial spring and set beside extensive arable farmlands to the north and west, along with flourishing horticultural zones in the hills to the east and south, Pella enjoyed a mild climate with plentiful winter rainfall, ideal for the mixed agriculture practiced in the MBA. The hills and plains surrounding the site were dotted with farmsteads and forts, small villages and fields, in a territorial unit that very probably stretched from the Jordan River to the arid uplands in the east.

Major trade routes, both east–west and south–north, crisscrossed this territory, linking Pella to both the Mediterranean coastlands and the Jordanian uplands. Indeed, so central was Pella placed in the Levantine trading network that it was recognized as the primary “gateway” community through which traded goods passed into Jordan from the Mediterranean world (Knapp, 1993). Numerous studies have emphasized the number and variety of foreign goods found at Pella through the ages. Long distance trade and/or contact is highlighted by the royal name scarabs from Tomb 62 (detailed below), centering on links between Pella and the Hyksos capital at Avaris in Egypt (Bourke & Eriksson, 2006). In the large chamber tomb associated with Tomb 106 “shackled man,” materials from Greece and Cyprus, Egypt, and Mesopotamia are evident (Bourke & Sparks, 1995). Further investigations of Pella’s MBA and Late Bronze Age (1550–1200 BCE) foreign relations emphasize links with Egypt,

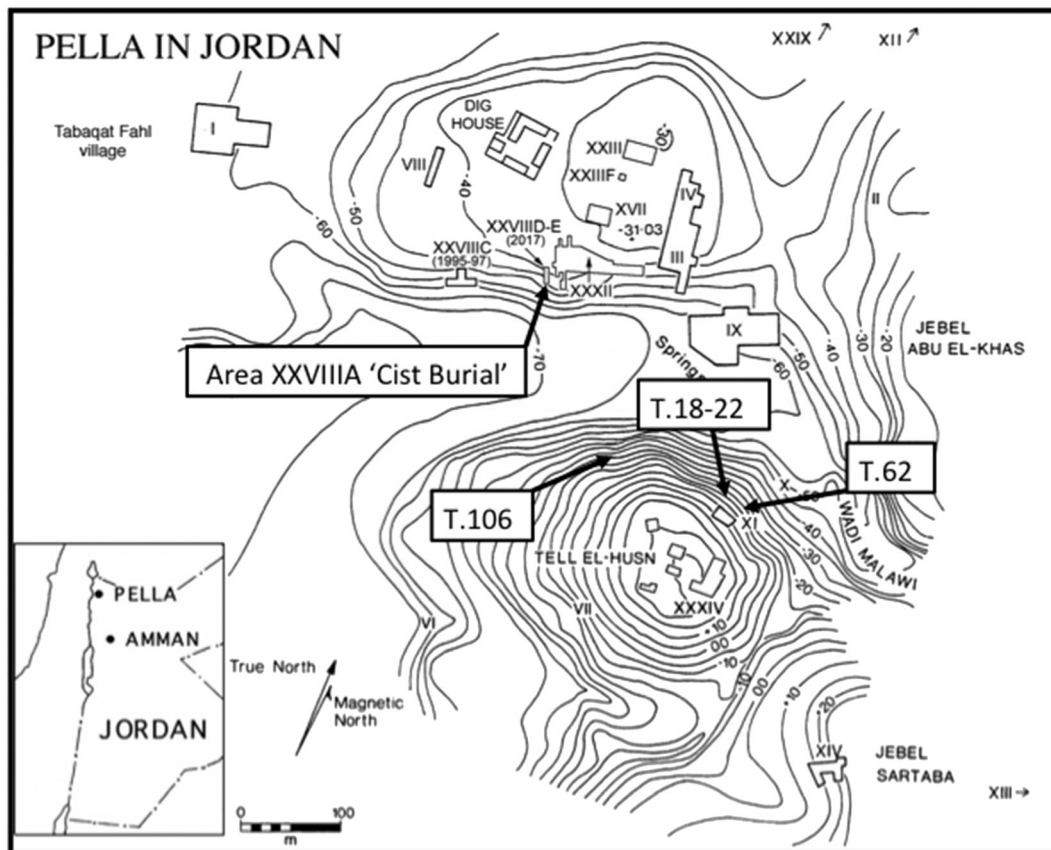


FIGURE 1 Map of Pella showing burials areas mentioned in-text. Inset of wider Jordan

Cyprus, and the Aegean, Mesopotamia, and Anatolia, sourcing much of the materials studied from tomb deposits such as examined in this study (Bourke et al., 2006).

This study integrates isotopic and biodistance data to explore whether Pella as a trade network also invited long-term settlement from people raised outside the local region, or if the contact and connections as a trade hub were “limited” to material exchange. With these two methodologies, detailed below, we can utilize human remains to explore both first-generation migration and ancestry and admixture. With inland Pella estimated as a key nodal site mediating trade between Egypt and the Jordanian uplands (Bourke & Eriksson, 2006; Knapp, 1993), this site provides valuable information about late MBA trade direction, intensity, and the varying strengths of nodal relationships. Given the quantity and variability of foreign goods, we hypothesize high first-generation migration as evidenced through isotopic analysis, but given that Near Eastern populations show genetic homogeneity across distinct cultural groups (Haber et al., 2017), we hypothesize little evidence of ancestry heterogeneity in our biodistance analysis. There are multiple ways to define the terms *mobility* and *migration*, but here, we define mobility as the capability to move, while migration is the actual movement following research (De Haas & Rodríguez, 2010).

2 | THE SITE OF PELLA

Occupation on the main mound of Khirbet Fahl and in the surrounding hinterland reached its pre-Classical peak during the MBA. A four-meter-thick mud-brick fortification wall, constructed in the early MBA around 1850 BCE, enclosed perhaps six hectares of the main mound, while forts and farmsteads dotted the near hinterland. The main cemetery area for MBA Pella spread across the sheer north face (Area XI) of the 60 m high, largely natural hill of Tell el-Husn, visible across the wadi to the south of the main settlement.

MBA burials in this main cemetery area consisted for the most part of ovoid single-chamber tombs, cut three to five meters back into the limestone bedrock of the north face. Some were found to be more or less intact, while others had been badly disturbed by millennia of erosion, often removing most of the original deposits and leaving no more than a “shelf” of in situ remains. All were affected by recurring water-damage to varying degrees, and the recorded positions of individual objects/skeletal elements need to be viewed in this light and regarded as tentative.

The University of Sydney excavated 10 tombs across this cemetery field during the 1980s (McNicoll et al., 1982, 1992), adding to the 10 excavated by the Jordanian Department of Antiquities (DAJ) in the 1960s (Bourke & Sparks, 1995), and two by Wooster College in 1979 (McNicoll et al., 1982). With one exception (discussed further below), most tombs contained up to 10 individuals, in what are assumed to be family groupings.

Excavators in Area XI encountered a cluster of four MBA tombs (Tombs 18–22) during the 1980 field season (Hennessy et al., 1981; McNicoll et al., 1982). The very large three-chambered Tomb 62 (also

Area XI), containing over 2000 objects, was excavated 20 m downslope to the east of the 1980 discoveries during the extended 1984 field season (McNicoll et al., 1992; Potts et al., 1985). During this same field season, excavations in Area XXVIII, located on the southern slopes of the settlement mound, uncovered an intramural stone-lined cist grave (F.10) containing two individuals, and many high-status grave goods (Potts et al., 1985). Finally, further work in the Area XI cemetery field in 1990 uncovered the *dromos* entranceway and external courtyard (Sydney Tomb 106), associated with a very large chamber tomb (DAJ Tomb 1), excavated by Jordanian archaeologists in 1963/1964 (Bourke & Sparks, 1995; Smith, 1973). The “shackled man” skeleton, the first of six individuals excavated over the course of the 1990–1992 field seasons, was found immediately east of the tomb entrance (Bourke et al., 1994; Bourke & Sparks, 1995; Walmsley et al., 1993).

2.1 | Husn cemetery area XI: Tomb 20 (MNI = 7)

Excavated in February 1980, Tomb 20 was approximately 3 × 4 m in extent, and bilobate in design (i.e., two 2 × 3 m areas partially divided from each other). Perhaps, 25% of the northern “lobe” and the entrance *dromos* to the tomb had been lost to erosion. The remains of seven individuals were recovered from the tomb floor, although none were articulated (Hennessy et al., 1981; McNicoll et al., 1982). Accompanying them were at least 99 registered grave goods. The high-quality ceramics, alabaster vessels, wooden inlays, metal pins, and jewelry items date to the MB IIC period, falling within the sixteenth century BCE.

2.2 | Husn cemetery area XI: Tomb 22 (MNI = 4)

Excavated in 1980 at the same time as nearby Tomb 20, Tomb 22 consisted of a single sub-round chamber approximately 2.5 × 2 m in extent (Hennessy et al., 1981; McNicoll et al., 1982). The northern side of the tomb had been somewhat affected by erosion and the entrance *dromos* removed. The remains of four individuals were recovered from the tomb floor, none articulated. Accompanying them were at least 27 registered grave goods. The ceramics are similar in quality to those from Tomb 20, although the range of grave goods is not as wide. The loosely associated poker-butt spearhead and tweezers are noteworthy, all suggesting a date somewhat earlier than Tomb 20, within the seventeenth century BCE.

2.3 | Husn cemetery area XI: Tomb 62 (MNI = 110)

Excavated between January and April 1984, Tomb 62 was among the largest MB-Late Bronze Age (LBA, ca. 1500–1200 BCE) period tombs ever discovered in the southern Levant (McNicoll et al., 1992; Potts et al., 1985). Located some 20 m east of the Tombs 20/22, Tomb 62 was cut more than eight meters into the bedrock face of Tell Husn

(Potts et al., 1985, fig. 5). The tomb consisted of a meter-long entrance dromos and three chambers, the first (Locus 1) roughly square and 3×4 m in extent. A meter-deep passageway (Locus 2) joined the first and second chambers, with Chamber 2 (Locus 3) more rounded and roughly 3.5 by 2.5 m in extent. Cut into the western wall of Chamber 2, the third chamber (Locus 4) was roughly apsidal in shape, and approximately 1.8 by 2 m in size. Although the tomb seemed intact, with little erosion damage evident, severe water churning of the rock-chambers was everywhere evident, with finds settling into visible bands of water-laid sediment and decomposed bone. Bone material was plentiful but crushed and fragmented to a remarkable degree, with pieces of more than 2 cm in size a rarity. From teeth and other identifiable fragments, initial estimates suggested somewhere between 100 and 150 individuals present in the tomb (McNicoll et al., 1992). Subsequent analysis of tomb content types may imply a slightly reduced number, perhaps around 110–120 individuals (Bourke, 2018).

The grave goods from within the three chambers numbered almost 2,200 in total, with more than 1,200 pottery vessels and nearly 1,000 stone, bone, wood, metal, glass, faience, and shell pieces (McNicoll et al., 1992). Most of the tomb contents are dated within the sixteenth and fifteenth centuries BCE. Grave goods are of variable quality, with some fine ceramics, especially the unrivaled collection of 95 Chocolate on White ware vessels, but overall, the precious metals and fine stonewares are few in number, leading excavators at the time of excavation to posit that this “tomb” may actually have been the collection-repository for a number of cleaned out chamber tombs (McNicoll et al., 1992).

Alternatively, contemporary very large tombs have been found at Shechem (Clamer, 1977), Jerusalem (North, 1965), Hazor (Yadin et al., 1960), Dothan (Cooley & Pratico, 1994), and Gezer (Seger & Lance, 1988), suggesting that large tombs with few precious metals and fine stonewares are not necessarily a rarity. While some tombs do contain gold and fine stonewares, most do not, so the failure to find these artifacts in Tomb 62 might simply reflect the quotidian lifeways of the population.

2.4 | Husn cemetery area XI: Tomb 106 “Shackled Man” burial (MNI = 6)

The assemblage designated “Tomb 106” came from a 7×5 m area located outside (north) of the meter-wide entrance passageway to DAJ Tomb 1, a very large (20×10 m) ovoid chamber tomb (Bourke et al., 1994; Bourke & Sparks, 1995; Walmsley et al., 1993). Although the two large chambers of Tomb 106 were previously excavated by Jordanian Department of Antiquities inspectors in 1964 (Bourke & Sparks, 1995; Smith, 1973), the entrance dromos and exterior frontage of the tomb were not. Sydney University cleared the exterior surfaces abutting the crumbling and unstable bedrock face outside DAJ Tomb 1, and a small part of the *dromos* passage itself in the 1990s (Bourke & Sparks, 1995, p. 166), but the great overburden of unstable crushed bedrock made significant excavation within the *dromos* itself too hazardous.

When the considerable quantities of crushed bedrock and erosion products were removed from the area of the tomb exterior, a line of three articulated skeletons, arranged head to toe, were found to stretch east along the bedrock exterior from the tomb entrance. The first of these skeletons, which closest to the entrance, was found to have a massive set of bronze shackles hammered onto his ankles (Figure 2) and has therefore been dubbed “the Shackled Man” (Bourke & Sparks, 1995). Excavators interpreted the collection of skeletal remains to be in some way associated with the closure of the tomb, perhaps representing retainer sacrifice, a rare but consistent presence in Bronze Age funerary rituals (Recht, 2018). Pottery (both local and Cypriot) and clay figurine fragments suggested a date within the fourteenth century BCE for the tomb entranceway “assemblage” (Bourke et al., 1994).

2.5 | Settlement mound area XXVIII: Trench A, F.10 “Cist Grave” (MNI = 2)

The “Cist Grave,” a stone-lined roughly rectangular burial pit some 2×1.5 m in extent, was excavated in February 1984 in the southwest field (Area XXVIII) of the main settlement mound (Bourke et al., 1994; Potts et al., 1985). The initial 5×5 m trench (expanded in later years) was situated on the extreme edge of the mound, placed there to investigate a large field-stone wall, and then suspected to be part of the Bronze Age fortification system. The grave was found sealed below Byzantine period stone paving and otherwise divorced from contemporary MBA period structural remains. The Cist Grave contained two fragmentary but apparently originally articulated adult burials. The burial deposit included 14 high status grave goods, consisting of seven fine ceramic vessels, a faience vase, two wood-inlay boxes, a scarab seal and a bronze toggle-pin, and two tortoise carapaces. In subsequent seasons of excavation (1986, 1992, and 1994), 12 individual neonate and young child burials were excavated, positioned in the near surrounds of the Cist Grave. All materials from the Cist Grave suggested a date within the Late seventeenth/early sixteenth century BCE for the burial, with the apparently associated neonate/young child burials broadly contemporary in date.

3 | ISOTOPE ANALYSES

Isotope analyses are powerful tools in archeological sciences, and past bioarcheological studies in the Levant and wider region have used them to investigate human diet and migration (e.g., Al-Bashaireh et al., 2010; Al-Shorman, 2004; Al-Shorman & El-Khoury, 2011; Stantis et al., 2020).

3.1 | Strontium ($^{87}\text{Sr}/^{86}\text{Sr}$)

Strontium isotope ($^{87}\text{Sr}/^{86}\text{Sr}$) analysis of human tissues provides insight into residential mobility and origin on the individual level,

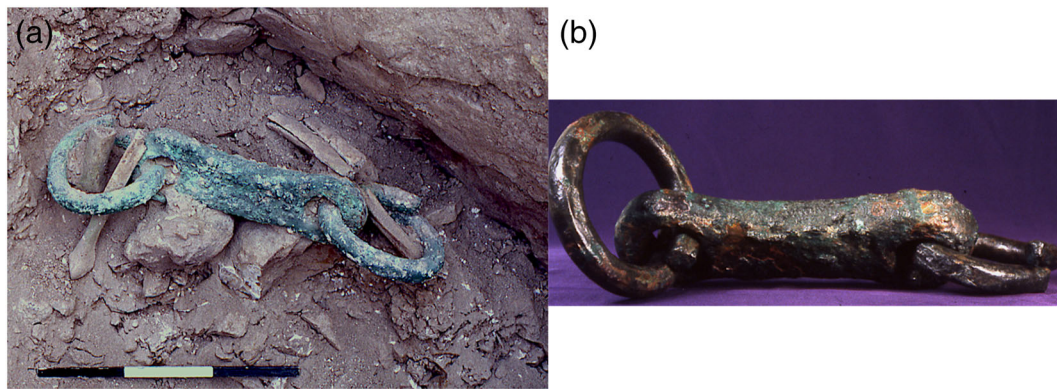


FIGURE 2 (a) Shackles in situ with tibiae and fibulae in the loops. (b) The shackles after restoration [Colour figure can be viewed at wileyonlinelibrary.com]

allowing extrapolations into large-scale socio-political dynamics (Sottysiak, 2019; Stantis & Schutkowski, 2019). Interpretation of strontium isotope analysis rests on the assumption that an individual's body tissues will reflect the $^{87}\text{Sr}/^{86}\text{Sr}$ values of the underlying geology in which they lived when these tissues were forming, with no appreciable fractionation across trophic levels or in metabolic processes (Lewis et al., 2017). Recent research suggests that fertilization with lime in modern agriculture affects interpretation of strontium isotopes (Thomsen & Andreasen, 2019), although that is not expected to be a major issue in Bronze Age Jordan as the soils surrounding Pella are lime-rich calciorthid soils (Lucke et al., 2014).

Multiple paleomobility studies have utilized $^{87}\text{Sr}/^{86}\text{Sr}$ on human dental enamel to identify non-locals in Jordan (Gregoricka et al., 2020; Judd et al., 2019; Perry et al., 2008, 2009, 2011; Sheridan & Gregoricka, 2015), including the analysis and collation of modern and archeological plant, animal, and soil samples to create a biospheric baseline (sometimes called an “isoscape”) for the country in order to understand the bioavailable strontium ratios within and between regions. This is preferred to a geological baseline, as human bioavailable strontium is obtained from plants, animals, and to a lesser extent drinking water, and thus, the bioavailable strontium in a region is not a direct reflection of the underlying geological substrate due to factors such as differential erosion of geological formations and atmospheric contributions (Henderson et al., 2009; Lewis et al., 2017).

3.2 | Oxygen ($\delta^{18}\text{O}$) and carbon ($\delta^{13}\text{C}$) from carbonate

Both $\delta^{13}\text{C}$ and $\delta^{18}\text{O}$ values are presented using delta values (δ) and expressed in per mill (‰) deviations relative to the international references standard Vienna Pee Dee Belemnite (VPDB), although $\delta^{18}\text{O}$ can also be presented relative to Vienna Standard Mean Ocean Water (VSMOW) (Sharp, 2017). $\delta^{13}\text{C}$ and $\delta^{18}\text{O}$ are given by $([R_{\text{sample}}/R_{\text{standard}}]-1) \times 1,000$, where R is $^{13}\text{C}/^{12}\text{C}$ or $^{18}\text{O}/^{16}\text{O}$, respectively.

Oxygen isotope ratios ($\delta^{18}\text{O}$) are a common tool for investigating individual movement (Chenery et al., 2010; Prowse et al., 2007). The

main intake of oxygen atoms into the body is through drinking water (Bryant & Froelich, 1995; Longinelli, 1984), and the difference in proportions between ^{18}O and ^{16}O is dependent largely on the climate (e.g., mean temperature and altitude) where this drinking water is sourced (Daux et al., 2008). Oxygen stable isotopes can be used to interpret paleomobility in the same way as $^{87}\text{Sr}/^{86}\text{Sr}$, but instead of reflecting the underlying geology, oxygen represents climate, latitude, altitude, and other factors (Pederzani & Britton, 2018).

$\delta^{13}\text{C}$ values can be used to differentiate between the consumption of terrestrial C_3 plants and C_4 /marine foods in past populations (DeNiro & Epstein, 1978; Lee-Thorp et al., 1989). C_3 plants, which include cereals such as wheat and barley as well as most cultivated fruits, vegetables, and legumes, display $\delta^{13}\text{C}$ values between -35% and -20% . Plants that use the C_4 (Hatch-Slack) photosynthetic pathway, such as maize, millet, and sorghum, display higher $\delta^{13}\text{C}$ values than terrestrial C_3 plants, typically between -16% and -9% (Sharp, 2017). C_4 plants are more heat tolerant than C_3 plants, because they are adapted to tropical and subtropical environments but do not thrive in arid environments without sufficient irrigation (Sage & Monson, 1998). With no C_4 crops (e.g., millet, sugarcane, and maize) cultivated in Jordan in the Middle Bronze Age and very few wild C_4 plants available for grazing animals in this region (Shoko et al., 2016), carbonate values are expected to reflect a C_3 -based diet.

3.3 | Diagenesis

Bone tissue readily re-equilibrates with its surrounding burial environment (Budd et al., 2000), so the erosional water damage to the human remains interred in Tomb 62 possibly leached strontium from bone and precipitated strontium from the groundwater and soil. Bone is highly susceptible to contamination from leaching, but dental enamel is more resistant to diagenetic effects due to its lower porosity and high inorganic composition (Chai et al., 2009; Hoppe et al., 2003; Lee-Thorp & van der Merwe, 1991). Proper pre-treatment allows us to confidently investigate migration using $^{87}\text{Sr}/^{86}\text{Sr}$ values from tooth enamel although it is still difficult to ascertain whether the dental

enamel sampled for this study have been diagenetically altered (Hoppe et al., 2003; Trickett et al., 2003).

FTIR (Fourier transformation infrared spectroscopy) analysis can be utilized for preservation assessment (France et al., 2020). Although $\delta^{18}\text{O}$ and $\delta^{13}\text{C}_{\text{carbonate}}$ can have preservation issues, especially surrounding recrystallization of the inorganic matrix, FTIR was not included in this study as spectroscopic indicators are not necessarily reliable for ascertaining the level of diagenetic changes (Trueman et al., 2008). Other methods for investigating diagenesis are available, notably trace element analysis (Kamenov et al., 2018). At a Mexican archeological site that displayed water-damage similar to Tomb 62, Pacheco-Forés et al. (2021) used trace element analysis of bone and tooth enamel to investigate diagenetic alteration of isotopic values. They suggest that non-locals who had original isotopic values outside the local biospheric range might now display values closer to, or within, the local range. Either these individuals' values were even further outside the local range before contamination or trace element analysis overestimated the isotopic resetting produced by diagenesis.

3.4 | Geological baseline

The geological evolution of Jordan during the Cenozoic has been dominated by the development of the Jordan Rift Valley. Prior to this, Paleozoic to Mesozoic marine sedimentation in the Tethys Ocean culminated in deposition of widespread Cretaceous limestone (Bender, 1975; Perry et al., 2008). Tectonic separation of Africa and Arabia that led to opening of the Red Sea to the south, propagated northwards as the Dead Sea plate boundary. Rather than proceeding to full oceanic spreading, this produced a trans-tensional rift valley, currently expressed as the Jordan Valley, running approximately north-south across the western Levant region (Shaw et al., 2003). The uplifted, eastern margin of this rift valley exposes rocks dating back to before the Paleozoic sedimentation, although the region around Pella exposes mainly the youngest, Cretaceous sediments from before Red Sea Rifting began. The Rift itself is filled with post-rift sediments, predominantly Quaternary material resulting from fluvial erosion and eolian sandstorms. Thus, the principal formations relevant to Pella are Cretaceous sediment, found mainly to the east and southeast, and Quaternary deposits, found mainly to the northeast.

Gregoricka et al. (2020) define five general geological regions in Jordan and defined biospheric $^{87}\text{Sr}/^{86}\text{Sr}$ value ranges for these regions with data from water, modern and archeological animals, and modern plants (Hartman & Richards, 2014; Hodell et al., 1990; Perry et al., 2008, 2011; Shewan, 2004; Stein et al., 1997). These geologic zones and ranges are summarized on Table 1. In the Jordan Rift Valley, Pella inhabitants might be expected to fall within $^{87}\text{Sr}/^{86}\text{Sr}$ ratios between 0.70782 and 0.70803. There is substantial overlap between the $^{87}\text{Sr}/^{86}\text{Sr}$ ratios of the wider Jordan Rift Valley, the Eastern Corridor, and one of the two Eastern Israeli Highland ranges.

TABLE 1 $^{87}\text{Sr}/^{86}\text{Sr}$ ranges estimated for different parts of Jordan. Data collated by Gregoricka et al. (2020)

	$^{87}\text{Sr}/^{86}\text{Sr}$ range(s)
Mediterranean coastal plains	0.70811–0.70925
Eastern Israeli highlands	0.70470–0.70690; 0.70790–0.70840
Jordan Rift Valley	0.70782–0.70803
Eastern corridor	0.70792–0.70814
Western highlands	0.70815–0.70834

3.5 | Climate, latitude, and altitude

Variation in modern mean annual $\delta^{18}\text{O}$ values of precipitation across the region principally occur in the south, where it is hotter and more arid, and in cooler regions such as mountain ranges (Bowen, 2018; Bowen et al., 2013). The estimated $\delta^{18}\text{O}$ mean value for annual precipitation at Pella is $-4.4\text{‰} \pm 0.3$ (Bowen, 2018; Bowen et al., 2013). However, the climate of Jordan has changed over time (Langgut et al., 2013), and the modern mean annual precipitation values cannot be expected to be representative of ancient values. It is also understood that precipitation was not the main source of drinking water in Pella, but nearby springs (Smith, 1973, pp. 88–90).

Although climate change might have altered expected $\delta^{18}\text{O}_{\text{dw}}$ values over time, large permanent springs appear to have been available as groundwater to inhabitants in the Pella region for thousands of years (Edwards, 2013). The Jordan River, though about 5 km from the site, was separated via a steep slope so likely not accessed regularly compared to the perennial spring that is assumed to be the primary source of water for Pella's inhabitants. No isotopic analyses have been conducted on groundwater near Pella, but hydrological studies have been carried out at aquifers and springs near Amman, to the southeast, and in northern Jordan. With considerations such as climate change, pollution, and differences in aquifer origin (sampling sites are approximately 25–50 km from Pella), these modern water values can, with caution, be compared to the human values gathered in this study. Groundwater $\delta^{18}\text{O}$ values collected near Amman averaged $-5.45\text{‰} \pm 0.4$ SD (VSMOW) (Grimmeisen et al., 2017). In the north, one aquifer system averaged $-4.64\text{‰} \pm 0.4$ SD, while an aquifer system with higher altitude recharge averaged $-6.03\text{‰} \pm 0.27$ SD (Obeidat et al., 2021).

Seasonal variation in rainfall contributes to changes in the expected biosphere isotopic values due to fluvial erosion from the surrounding ranges and dust storms. For humans, this should average out over time, even with the smaller samples of enamel “capturing” shorter time periods of tooth modeling. For short-lived plants and animals such as those collected for the baseline, these seasonal events could affect values, although no oxygen stable isotope baseline samples were collected for this study.

4 | DENTAL NONMETRIC TRAITS AND BIODISTANCE

The isotope analysis was complemented by exploring another aspect of bioanthropological analysis, biological distance (bio-distance) analysis, which estimates the (dis)similarity of individuals and groups based genetic or phenetic information (Stojanowski & Schillaci, 2006). Phenotypic characteristics are physical expressions of genetic traits in interaction with environmental factors, resting on the assumption that physical similarity indicates underlying biological closeness (Hefner et al., 2016; Stojanowski & Schillaci, 2006). As the effect of extrinsic factors to phenotypic expression varies between different skeletal features, not all can be considered equally useful for biodistance analyses (Hefner et al., 2016).

Dental morphology has been used to infer biological closeness, recording variation in the grooves and cusps of molars as well as roots. While tooth ontogeny, governed by an estimation of 300 different genes, is also affected by environmental factors, the process is still predictable and becoming increasingly well-understood (Rozzi, 2016; Thesleff, 2006, 2014; Townsend et al., 2009, 2012). This makes teeth one of the most reliable sources for non-metric biodistance analysis. Though there are several methods for recording dental nonmetric shape variation (e.g., Alt & Vach, 1995; Zoubov, 2011), the Arizona State University Dental Anthropology System (ASUDAS henceforth) has by far been the most widely employed method. Over 40 traits have been included in the standard, described at length in several dedicated publications (Scott & Irish, 2017; Scott, Pilloud, et al., 2018; Scott & Turner, 1997; Scott, Turner, et al., 2018), chosen for their durability, lack of sexual dimorphism, and heritability. Twin and genetic studies have produced similar patterns of biological closeness (Delgado et al., 2019; Hubbard et al., 2015).

Dental non-metric traits have been used to explore both intra- and inter-regional differences in Near Eastern sites (Alexanderson, 1978; Bentley, 1987; Dicke-Toupin, 2012; Elias, 2016; Lovell & Scott Haddow, 2006; Nassar, 2010; Özbek, 1975; Parras, 2004; Sottysiak & Bialon, 2013; Ullinger et al., 2005). These studies have used either pair-wise comparisons of traits between sites or Mean Measure of Divergence (MMD), a multivariate statistical tool that employs all trait frequencies together to compare sites. Though MMD can accommodate missing data due to its use of frequency tables, small sample sizes can hinder the analysis. Furthermore, because trait frequencies are acquired by grouping the data, we lose the individuals. With the Pella sample in question, the sample is not only small in size, but isotope values and dental morphology could only be linked via singular teeth if individuals are kept discrete.

Though there are some options to explore individuals through biodistance, missing data limit those options. Gower similarity coefficient has been employed to explore biodistance, allowing for some missing data in archeological datasets (Ricaut et al., 2010; Stojanowski & Schillaci, 2006). Comparison of genetic data to

biodistance data acquired from a Gower distance matrix showed similar results (Stojanowski & Hubbard, 2017).

5 | MATERIALS

To reduce the chances of double-sampling the same individual, within each level of a tomb, the most frequently occurring permanent second molars (i.e., upper left, lower left, upper right, or lower right) would be selected with second lower left molars preferentially chosen, especially in the highly commingled context of Tomb 62. With few exceptions, these teeth were isolated or extracted from jaw fragments, and so age and sex estimations were not possible. Teeth with closed apices were preferred, with mesial root apices expected to be closing around 9.5–15 years of age (Moorrees et al., 1963), although many teeth had broken at the CEJ with only the crown observable and so often root closure could not be assessed. The Pella Middle Bronze Age individuals sampled for this study are curated at the University of Sydney (Australia). Despite the limitations owing to the poor preservation and commingled nature, 22 permanent second molars were collected: 17 samples from Tomb 62, 2 from Tomb 106, and 1 each from Tomb 20, Tomb 22, and the cist grave of Trench XXVIII, F.10.

No baseline samples specific to Jordan or the more specific region were available for collection for this project. However, Perry et al. (2008) collected and analyzed rodent teeth from several Jordanian sites, including Pella. Rather than using only Pella baseline samples, rodents Perry and colleagues collected from nearby Ya'amun and Bediyeh are also integrated to expand the baseline to represent the nearby Quaternary and Cretaceous geological formations to the northeast and east as the strontium isoscape. Two grass samples collected by Shewan (2004) for use as a baseline of the nearby Natufian settlement of Wadi Hammeh 27 could be integrated into the biospheric baseline. However, with no other plant data, there is concern that ratios from these two samples would be too specific to their small area and not representative of the wider range of ratios that humans would have utilized as their range. So only the animal samples are used to define local values for this research. No $\delta^{18}\text{O}$ proxies specific to the region are currently available in the literature.

The rodent enamel samples collected by Perry et al. (2008) will be used to create a local baseline for $^{87}\text{Sr}/^{86}\text{Sr}$ ratios. The median \pm 1.5 IQR of $^{87}\text{Sr}/^{86}\text{Sr}$ ratios of rodent enamel samples from Pella, Ya'amun, and Bediyeh will serve as local values, and any Pella individuals outside of these values will be considered “non-local.” The rodent enamel $^{87}\text{Sr}/^{86}\text{Sr}$ ratios from Perry et al. (2008) show a range of values between 0.70792 and 0.70801, with a median of 0.708012 (0.000395 \pm 1.5*IQR). These values are similar to the expected range for the Jordan Rift Valley estimated by Gregoricka et al. (2020), 0.70782–0.70803. To compare the $\delta^{18}\text{O}$ values from enamel carbonate to predicted drinking water values, $\delta^{18}\text{O}_{\text{dw}}$ values are calculated using the equation from Chenery et al. (2012) that utilizes eq. 6 from Daux et al. (2008).

6 | METHODS

6.1 | Isotopic analysis

Initial sample preparation was conducted in the Department of Archaeology and Anthropology Dorset House laboratory at Bournemouth University (United Kingdom). After burring to remove the outer surface, enamel was removed from the tooth using a dental cutting instrument with a rotary saw attachment. Any dentine attached was gently burred. The enamel was separated for strontium and $\delta^{18}\text{O}/\delta^{13}\text{C}$ analyses.

Analytical methods were conducted in the Department of Earth Sciences at Durham University (United Kingdom). The sample for $\delta^{18}\text{O}$ and $\delta^{13}\text{C}$ analyses was powdered in an agate mortar and pestle and then pretreated with 0.1 M acetic acid at room temperature for no longer than 4 h. The powder was then rinsed three times with ultrapure water and then dried in a 50° oven overnight. Carbon ($\delta^{13}\text{C}$) and oxygen ($\delta^{18}\text{O}$) isotope ratios were measured in the carbonate (CO_3) component of tooth enamel following the procedures of Bentley et al. (2007). For each tooth, approximately 2 mg of powdered sample was reacted with 99% ortho-phosphoric acid for 2 h at 70°C. CO_2 was then separated from helium in the resultant gas mix using a Thermo Fisher Scientific Gasbench II and passed into a Thermo Fisher Scientific MAT 253 gas source mass spectrometer for isotopic analysis. Replicate analysis of two samples yielded a greatest difference of 0.17‰ for $\delta^{13}\text{C}$ and 0.11‰ for $\delta^{18}\text{O}$. In each run, the international reference materials NBS 19 ($n = 3$), IAEA-CO-1 ($n = 3$), and LSVEC ($n = 3$) were analyzed along with two internal standards: a carbonate DCS01 ($n = 7$) and a composite tooth enamel Dobbins ($n = 2$). All standards yielded an analytical reproducibility better than 0.26‰ (2 SD) for $\delta^{13}\text{C}$ and 0.70‰ (2 SD) for $\delta^{18}\text{O}$. All values have been normalized to the accepted values of +2.49‰ VPDB and -46.6‰ VPDB for $\delta^{13}\text{C}$, and -2.40‰ VPDB and -26.70‰ VPDB for $\delta^{18}\text{O}$, for IAEA-CO-1 and LSVEC, respectively.

After being sonicated and rinsed three times with MilliQ water, the strontium samples were purified using the ion exchange method outlined by previous research (Cavazzuti et al., 2019; Smits et al., 2010). The cleaned enamel samples were weighed, dissolved in concentrated HNO_3 , and then diluted to 3 M HNO_3 . The sample solutions were then loaded onto columns with Eichrom Sr-spec resin, eluted with MilliQ water, and acidified to 3% HNO_3 for analysis. Strontium isotope ratios were measured using a ThermoFinnigan Multi-collector ICP Mass Spectrometer (MC-ICP-MS). Run over 4 days, reproducibility of the standard NBS987 during sample analysis was 0.710249 ± 0.000004 (2SD, $n = 57$). All NBS987 values have been normalized to the accepted value of 0.710240 (Johnson et al., 1990; Terakado et al., 1988).

6.2 | Dental nonmetric data collection

Because the Pella material was mostly represented by loose, commingled teeth, the “individuals” of this analysis become

represented by a single tooth rather than an entire dental arcade. This limited the collection of dental traits to the second lower molars, the most frequent tooth used in the stable isotope study.

The dental traits used in the analysis were anterior fovea (AF), groove pattern y (GP_y), cusps 5–7 (C5, C6, C7), mesial and distal trigonid crest (MDTC), and protostylid (PR). All traits except groove pattern were recorded on a degree of expression, following Scott and Irish (2017). Groove pattern “Y” was recorded as present (1) while patterns “X” and “+” were absent (0). An additional trait, mandibular molar pit tubercle (MPT) was also recorded. Though the trait is not currently part of ASUDAS, recent research has indicated great potential for the trait (Marado & Silva, 2016; Weets, 2009). The trait was scored according to the protocol proposed by Marado and Silva (2016).

Traits exhibiting no variation in the data set (0% frequency for C6, C7, and MDTC) were excluded from further testing. Kendall's tau-b test indicated no strong inter-trait correlation between the remaining traits ($b \geq 0.5$). All teeth were recorded by NM to avoid inter-observer error. Intra-observer tests indicated good agreement between observation events (Maaranen et al., 2019). Any teeth with notable occlusal wear (greater than 3 on the Smith, 1984 scale) were not recorded for nonmetric traits.

6.3 | Statistical analysis

Isotopic data were managed using isotopes data management practice recommended by the IsoArch association for future metadata analysis (Salesse et al., 2018). All statistical analyses were performed using R (R Core Team, 2000).

Two methods are employed to identify non-locals: biospheric $^{87}\text{Sr}/^{86}\text{Sr}$ data and bagplot visualization of both $^{87}\text{Sr}/^{86}\text{Sr}$ and $\delta^{18}\text{O}$ data from the human enamel. Individuals outside of the rodent enamel median ± 1.5 IQR (i.e., those with ratios below 0.707617 or above 0.708407) are identified as potential non-locals using $^{87}\text{Sr}/^{86}\text{Sr}$ alone. With no contemporaneous local $\delta^{18}\text{O}$ values, a bagplot of $^{87}\text{Sr}/^{86}\text{Sr}$ and $\delta^{18}\text{O}$ values for the Pella individuals will be used as an additional tool for identifying non-locals. Bagplots are two-dimensional box plots that help visualize outliers in a dataset (Rousseeuw et al., 1999). This method is statistically robust and recommended for multi-isotopic analyses of paleomobility (Lightfoot & O'Connell, 2016; Stark et al., 2020). Bagplots can be used to visually identify where data points sit within three nested polygons, the “bag,” “fence,” and “loop.” The bag is the innermost polygon, formed around the depth median with upwards of half of data points ($\leq n/2$) that form the smallest area. The “fence” polygon is formed by magnifying the bag by a factor of 3; it will not be drawn on the bagplot, but data points outside this fence are considered statistical outliers and will be highlighted. The “loop” polygon, the area between the bag and fence, is shaded, and individuals within this area are noted as not being as close to the median as those data points within the bag, but also not outliers. The bagplot was created using the `aplpack` package from R (Wolf & Bielefeld, 2019).

Biodistance analysis was completed using Gower distances from the R package cluster (Maechler et al., 2019) which allows for mixed data sets and missing values, an issue with most archeological material. The function also allows for missing values but only circa 30% in the investigator's experience. "Individuals" with more than 30% missing values (i.e., teeth where too many traits could not be scored due to wear) were excluded from the analysis. The function cluster allows the investigator to distinguish variable types. Anterior fovea and cusp 5 had multiple levels, while groove pattern had been dichotomized based on the pattern "Y." As the traits protostylid and mandibular molar pit tubercle were only recorded on the grade 1, they were typed as binary variables.

The resulting distance matrix was analyzed for morphology using partitioning around medoids (PAM). The optimal number of groups was assessed using silhouette width which measures similarity between clusters by their observations. The groups were further visualized using *t*-distributed Stochastic Neighbor Embedding (*t*-SNE) which reduces high-dimensional data by constructing a probability distribution over pairs of high-dimensional observations and then transforming them into a similar probability distribution. This was done using the R package Rtsne (van der Maaten & Hinton, 2008).

The R code and the dataframes needed to duplicate all statistical tests and data visualization from this research are available as supporting information (Data S1–S3).

7 | RESULTS

The isotopic data are presented on Table 2 and summarized on Table 3. The $^{87}\text{Sr}/^{86}\text{Sr}$ data are not normally distributed ($W = 0.575$, $p < 0.001$), while the $\delta^{13}\text{C}$ ($W = 0.961$, $p = 0.515$) and $\delta^{18}\text{O}_{\text{VPDB}}$ ($W = 0.967$, $p = 0.645$) data are normally distributed.

Strontium ratios range from 0.70619–0.70845, with a median value of 0.70815 (IQR 0.00014). Nineteen of the 22 individuals

TABLE 3 Statistical summary of Pella isotopic data

	Median	IQR	<i>n</i>
$^{87}\text{Sr}/^{86}\text{Sr}$	0.70815	0.00014	22
	Mean	SD	<i>n</i>
$\delta^{18}\text{O}$	−4.18	0.81	22
$\delta^{13}\text{C}$	−12.35	0.41	22

TABLE 2 Strontium, carbon, and oxygen isotope values from dental enamel at the site of Pella

Project context details	$^{87}\text{Sr}/^{86}\text{Sr}$	Error	$\delta^{13}\text{C}_{\text{carb}}$	$\delta^{18}\text{O}_{\text{carb}}$	Tooth (FDI)	Lab ID
Area XI: Tomb 106 locus 1.11. 'Shackled man'	0.708148	9.00E−06	−12.19	−4.35	47	1039
Area XXVIII: Trench A. F. 10 locus 1.10 'cist grave'. Skull of skeleton 2	0.708136	7.00E−06	−12.39	−5.64	47	1040
Area XI: Tomb 106 locus 1.11. 'Shackled man'	0.708072	8.00E−06	−12.27	−3.58	47	1041
Area XI: Tomb 62 locus 1.3	0.70845	1.00E−05	−12.09	−3.91	37	1042 ^a
Area XI: Tomb 62 locus 1.2	0.708157	1.00E−05	−11.68	−4.85	37	1043
Area XI: Tomb 62 locus 1.7	0.708286	6.00E−06	−12.14	−4.5	37	1044
Area XI: Tomb 62 locus 1.5	0.70819	1.00E−05	−11.78	−4.09	37	1045
Area XI: Tomb 62 locus 1.7 tooth 1 of 2	0.706185	8.00E−06	−12.39	−3.92	37	1046 ^{a,b}
Area XI: Tomb 62 locus 1.7 tooth 2 of 2	0.706836	8.00E−06	−12.49	−4.71	37	1047 ^{a,b}
Area XI: Tomb 62 locus 3.4	0.708128	7.00E−06	−11.73	−3.89	37	1048
Area XI: Tomb 62 locus 3.4	0.708196	7.00E−06	−12.93	−2.23	37	1049 ^b
Area XI: Tomb 62 locus 4.4 tooth 1 of 3	0.708145	7.00E−06	−12.78	−3.53	37	1050
Area XI: Tomb 62 locus 4.4 tooth 2 of 3	0.707744	8.00E−06	−12.5	−4.53	37	1051
Area XI: Tomb 62 locus 4.4 tooth 3 of 3	0.708211	8.00E−06	−12.63	−5.04	37	1052
Area XI: Tomb 62 locus 3.4 tooth 1 of 3	0.70826	1.00E−05	−12.82	−4.06	37	1053
Area XI: Tomb 62 locus 3.4 tooth 2 of 3	0.70822	1.00E−05	−12.58	−3.56	37	1054
Area XI: Tomb 62 locus 3.4 tooth 3 of 3	0.707965	8.00E−06	−12.88	−4.47	37	1055
Area XI: Tomb 62 locus 3.4	0.708286	8.00E−06	−11.86	−3.93	37	1056
Area XI: Tomb 20 locus 1.1 'skull C'	0.708082	8.00E−06	−12.01	−3.2	27	1057
Area XI: Tomb 22 locus 2.1	0.708057	8.00E−06	−13.01	−4.35	27	1058
Area XI: Tomb 62 locus 3.6 tooth 1 of 2	0.708212	8.00E−06	−12	−3.68	37	1059
Area XI: Tomb 62 locus 3.6 tooth 2 of 2	0.708239	8.00E−06	−12.54	−5.99	37	1060

^aIndividuals identified as non-locals using biospheric $^{87}\text{Sr}/^{86}\text{Sr}$ values.

^bIndividuals identified as non-locals using bagplot analysis.

display $^{87}\text{Sr}/^{86}\text{Sr}$ ratios reflecting the local baseline (Figure 3). All outliers are from Tomb 62, Locus 1. The two individuals displaying the lowest $^{87}\text{Sr}/^{86}\text{Sr}$ values in the assemblage are from Level 1.7, while the other outlier, with the highest $^{87}\text{Sr}/^{86}\text{Sr}$ in the assemblage, is from Level 1.3.

$\delta^{18}\text{O}$ values range between -5.99‰ and -2.23‰ , with a mean value of -4.18‰ (± 0.81 SD). $\delta^{13}\text{C}$ values range from -13.01‰ to -11.68‰ with a mean value of -12.35‰ (± 0.41 SD). The non-locals identified using the strontium biospheric range show $\delta^{18}\text{O}$ and $\delta^{13}\text{C}$ values clustering with most of the samples (Figure 4). When converted to $\delta^{18}\text{O}_{\text{dwt}}$, Pella values range between -9.3‰ and 3.14‰ , with a mean of -6.34 (± 1.33 SD).

Using the bagplot to identify statistical outliers using both $^{87}\text{Sr}/^{86}\text{Sr}$ and $\delta^{18}\text{O}$ (Figure 5), the two outliers with low $^{87}\text{Sr}/^{86}\text{Sr}$ remain as statistical outliers but the individual with the highest $^{87}\text{Sr}/^{86}\text{Sr}$ is within the loop polygon and not an outlier. One individual is an outlier along the $\delta^{18}\text{O}$ axis, the individual with the highest $\delta^{18}\text{O}$ value within the dataset. This outlier, like those with “non-local” $^{87}\text{Sr}/^{86}\text{Sr}$ values, is from Tomb 62.

A matrix of Gower distances was created using 13 individuals and five dental traits (Table 4). Cluster analysis indicated best division into four clusters with a silhouette width measure of 0.6, suggesting moderate structure. The visual output of the PAM clusters indicates similar clustering in two-dimensional space (Figure 6). Hierarchical cluster



FIGURE 3 $^{87}\text{Sr}/^{86}\text{Sr}$ values of all individuals sampled from Bronze Age Pella. Shaded rectangle represents the biospheric local range derived from Perry et al. (2008) [Colour figure can be viewed at [wileyonlinelibrary.com](https://onlinelibrary.wiley.com)]

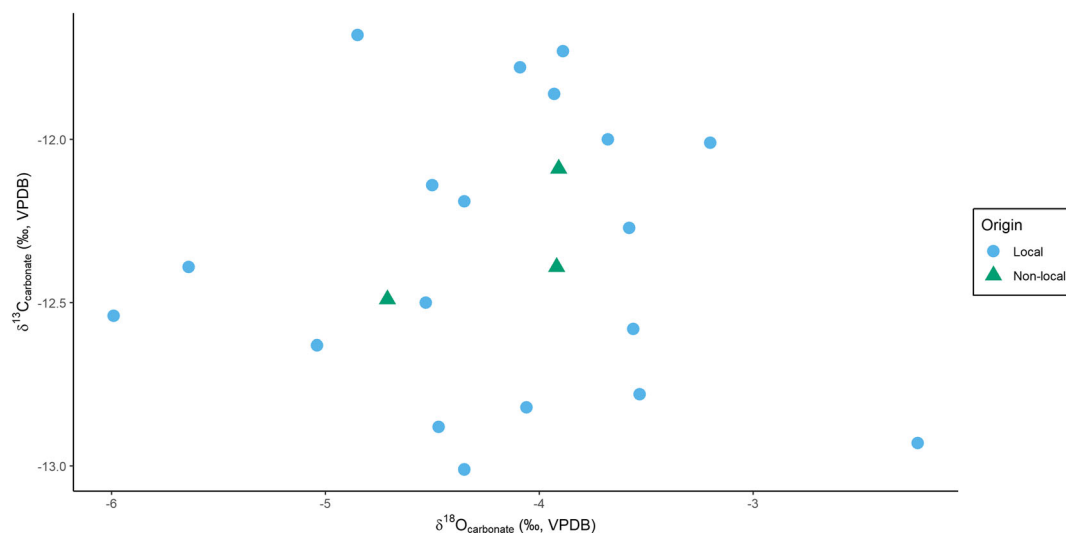


FIGURE 4 $\delta^{18}\text{O}$ and $\delta^{13}\text{C}$ values from carbonate of all individuals sampled from Bronze Age Pella. Nonlocals are individuals identified as outliers in the $^{87}\text{Sr}/^{86}\text{Sr}$ analysis [Colour figure can be viewed at [wileyonlinelibrary.com](https://onlinelibrary.wiley.com)]

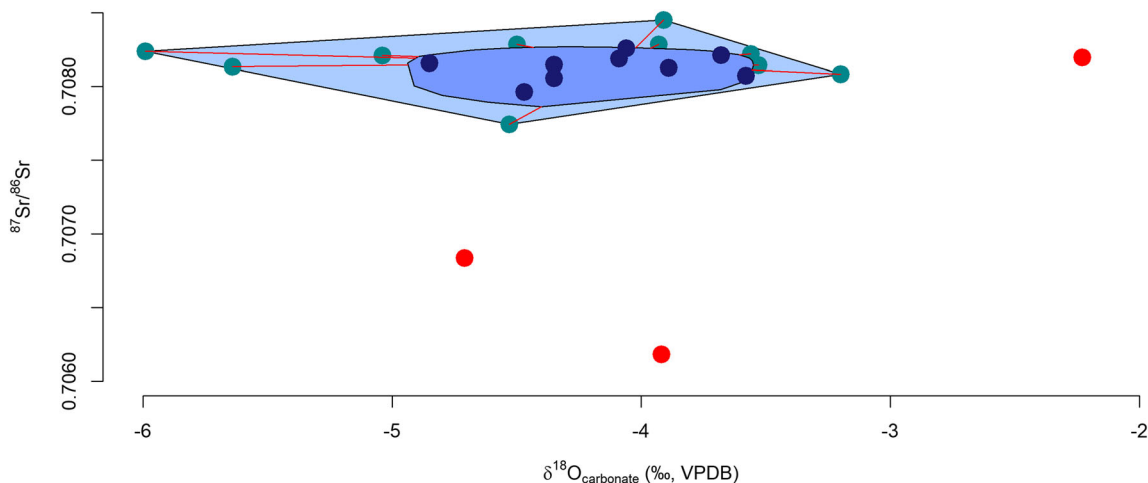


FIGURE 5 Bagplot analysis of $\delta^{18}\text{O}$ and $^{87}\text{Sr}/^{86}\text{Sr}$ values. The innermost polygon (“bag”) and individuals within that polygon are shaded in midnight blue, while the “loop” polygon and individuals within it are in lighter teal. The “fence” polygon is not shaded, but three outliers are denoted in red [Colour figure can be viewed at wileyonlinelibrary.com]

TABLE 4 Pella dental trait scores

Project context details	Lab ID	Plot ID	AF	GP_y	C5	PR	MPT
Area XXVIII: Trench A. F. 10 locus 1.10 “cist grave.” Skull of skeleton 2	1040	28	1	1	0		
Area XI: Tomb 106 locus 1.11. ‘Shackled man’	1039	106		1	0	1	1
Area XI: Tomb 62 locus 1.3	1042	62.1	0	0	0	1	0
Area XI: Tomb 62 locus 1.5	1045	62.1E	1	1	3	1	0
Area XI: Tomb 62 locus 1.7 tooth 2 of 2	1047	62.1GF.2	1	0		0	0
Area XI: Tomb 62 locus 3.4	1049	62	2	0	3	1	0
Area XI: Tomb 62 locus 4.4 tooth 1 of 3	1050	62.4D.1		0	3	1	0
Area XI: Tomb 62 locus 4.4 tooth 2 of 3	1051	62.4D.2	2	1		1	0
Area XI: Tomb 62 locus 3.4 tooth 1 of 3	1053	62.3D.842.1	0	0		0	0
Area XI: Tomb 62 locus 3.4 tooth 3 of 3	1055	62.842.3D.3	0			1	1
Area XI: Tomb 62 locus 3.4	1056	62.3D.842069	0	1	0	1	1
Area XI: Tomb 62 locus 3.6 tooth 1 of 2	1059	62.3F.1	1	0		1	0
Area XI: Tomb 62 locus 3.6 tooth 2 of 2	1060	62.3F.2	2	0	0	1	0

Note: Dental trait abbreviations stand for anterior fovea (AF), groove pattern γ (GP_y), cusp 5 size (C5), protostylid (PR), and mandibular molar pit tubercle (MPT).

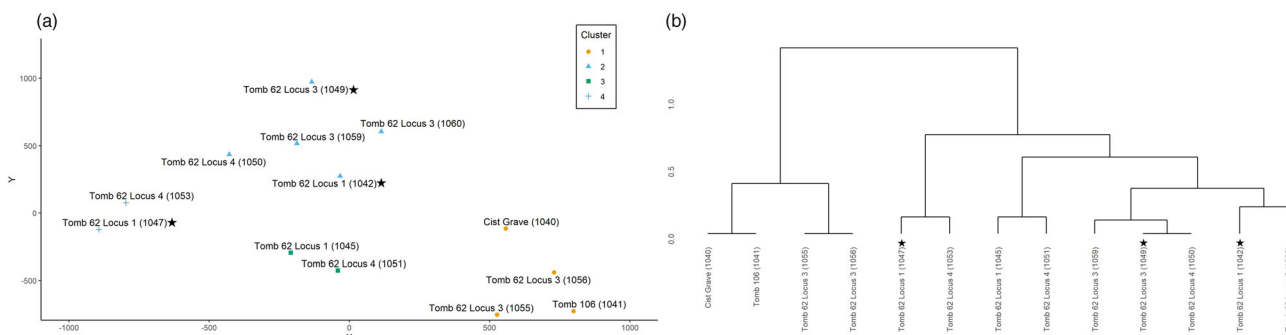


FIGURE 6 Plots of Pella data by clusters indicated by both partitioning around medoids (a) and hierarchical clusteranalysis (b). Abbreviations of individuals from Table 4. ★ denotes a non-local isotopically [Colour figure can be viewed at wileyonlinelibrary.com]

analysis produced the exact same groups for the data (Figure 6). Tomb 62 commingled individuals were divided across all morphological groups, while the two primary Middle Bronze Age burials (106 and XXVIII) grouped together. The $^{87}\text{Sr}/^{86}\text{Sr}$ and $\delta^{18}\text{O}$ isotopic values of the individuals assigned clusters are visualized in Figure S2.

7.1 | Discussion

Regarding $^{87}\text{Sr}/^{86}\text{Sr}$ values, we defined a more broad local isocape by using the median \pm 1.5 IQR rather than the range of rodent enamel $^{87}\text{Sr}/^{86}\text{Sr}$ values. Given the small comparative size currently available, a more conservative estimate of who was non-local seemed prudent. Two of the non-locals identified using $^{87}\text{Sr}/^{86}\text{Sr}$ local biosphere ratios (and identified as non-locals with the bagplot) display lower $^{87}\text{Sr}/^{86}\text{Sr}$ ratios relative to the rest of the assemblage. Plant and animal samples from the basalts/pyroclastic rocks of the Golan Heights (Hartman & Danin, 2010; Shewan, 2004) show similar ratios; this could suggest a northern origin for these two individuals. The individual with the highest $^{87}\text{Sr}/^{86}\text{Sr}$ ratio in the collection shows values aligned with the Mediterranean coast (Gregoricka et al., 2020). However, there are plenty of understudied regions in the Levant regarding $^{87}\text{Sr}/^{86}\text{Sr}$ analysis, such as the Sinai Peninsula or eastern Jordan.

When comparing modern groundwater $\delta^{18}\text{O}$ values with the $\delta^{18}\text{O}_{\text{dw}}$ of the Pella individuals, Pella people show lower values on average $-6.34 (\pm 1.33 \text{ SD})$ compared to the modern annual mean precipitation ($-4.4\text{‰} \pm 0.3$) and modern groundwater ($5.45\text{‰} \pm 0.4$ in Amman, $-4.64\text{‰} \pm 0.4$ and $-6.03\text{‰} \pm 0.27$ in Northern Jordan). The perennial spring Pella's inhabitants relied on may have recharged from higher altitude, cooler average temperature, or with less anthropogenic contamination than the modern data collected.

In a previous study, Pella individuals from the Iron Age (ca. 1200–550 BCE) were analyzed for $\delta^{18}\text{O}$ values from the phosphate portion of enamel (Alakkam, 2002). When converted to enamel carbonate values using the equation by Chenery et al. (2012), these Iron Age individuals display similar $\delta^{18}\text{O}$ (VPDB) values to the Bronze Age group analyzed in this study (mean -4.6‰ , $n = 25$ individuals). This might suggest similar oxygen stable isotope values in drinking water over the Bronze and Iron Ages.

The three individuals with $^{87}\text{Sr}/^{86}\text{Sr}$ values outside the local isocape display $\delta^{18}\text{O}$ values clustering within the rest of the assemblage. This suggests these non-locals originate from a region with a different $^{87}\text{Sr}/^{86}\text{Sr}$ biosphere from Pella, but climatic conditions that created similar $\delta^{18}\text{O}_{\text{dw}}$ values. As per usual, isotopic investigation of migration is better utilized to identify non-locals than in identifying the origin of these non-locals.

All individuals identified as non-locals, using the biospheric values or the bagplot, are from Tomb 62. This might simply be a sampling issue, with 17 of the 22 individuals (77%) analyzed belonging to Tomb 62. The two individuals with $^{87}\text{Sr}/^{86}\text{Sr}$ ratios below the local baseline (i.e., below 0.707617) also identified as outliers using the bagplot (Laboratory IDs 1046 and 1047), as are the two individuals with the highest and lowest $\delta^{18}\text{O}$ values in the assemblage. Both individuals

display $^{87}\text{Sr}/^{86}\text{Sr}$ values within the local values. This could be a result of these individuals hailing from areas with similar geological values (such as anywhere up and down the Jordan Rift Valley), but from a region with a different climate that altered their drinking water oxygen isotope composition during life. With major altitude changes in this region of Jordan, the uplands with a colder climate and higher altitude could be a potential place of origin for the individual displaying the lower $\delta^{18}\text{O}$ value.

The issue of equifinality needs to be addressed, how the end state (in this instance, the $^{87}\text{Sr}/^{86}\text{Sr}$ ratios from dental enamel) can be attained by many different means, that is, that the $^{87}\text{Sr}/^{86}\text{Sr}$ ratios found in the “local” individuals can actually be acquired not only by living locally, but also by living in areas with a similar $^{87}\text{Sr}/^{86}\text{Sr}$ biospheric range (Stantis et al., 2015; Torrence, 1986; Torrence et al., 1992). While 19 of the 22 individuals analyzed displayed $^{87}\text{Sr}/^{86}\text{Sr}$ ratios aligning with local values in the Jordan Rift Valley and the Eastern corridor, these values also align with biospheric ranges in parts of the Mediterranean coast, Eastern highlands, and Western highlands (Figure 7).

One of individual with local $^{87}\text{Sr}/^{86}\text{Sr}$ ratio (Laboratory ID 1049) was identified as a likely non-local using the bagplot with $\delta^{18}\text{O}$ data, highlighting the need for multiple pieces of data to inform assessing mobility and migration in the past. Given the commingled nature of the tombs (common in Levantine Bronze Age burial practice, even when the tombs are not severely water-churned as in the case of Tomb 62), archeological proxy evidence for movement is difficult to utilize, but osteological evidence of movement could have value.

The issue of diagenetic contamination also needs to be addressed, especially in Tomb 62. Tooth enamel is more resistant to post-depositional alteration than bone (Budd et al., 2000; Hoppe et al., 2003) but not completely immune to the effects. Furthermore, strontium is more tightly bound to the crystalline structure of enamel compared to oxygen from carbonate. Nonetheless, diagenesis might have altered values to be closer to or within local biospheric ranges. There might have been more individuals displaying non-local isotopic values without the potential water-related alterations in Tomb 62.

In this study, we rely on bagplot analysis for identification of non-locals within this assemblage until the creation of a more robust biosphere encompassing multiple isoscapes with a wider sampling strategy, and this method has limitations. Non-locals in an assemblage have often been recognized as those individuals falling two standard deviations outside the population mean in geographic areas without established biospheric data (Bentley et al., 2003, 2004; Price et al., 2002; Stantis et al., 2016). This method, however, has often been considered less satisfactory as the mean might not represent the local biosphere and two standard deviations (estimated to cover 95% of a given dataset) might encompass non-local values as well as local individuals. This issue also applies to bagplot analysis, although the use of median and IQR is preferable to mean and standard deviation with non-normally distributed data, which archeologically derived isotopic data often is (Price et al., 2002, 2008).

Given the geographical spread and great time-depth of occupation in Jordan, isotopic studies of paleomobility are still nascent in the

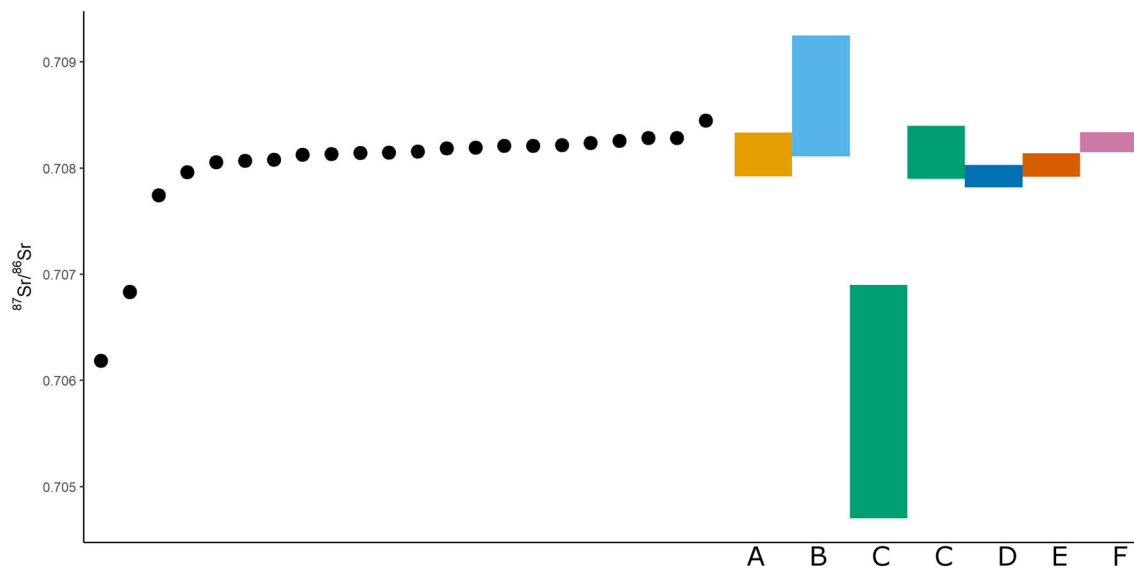


FIGURE 7 $^{87}\text{Sr}/^{86}\text{Sr}$ values of Bronze Age Pella individuals plotted with “local” biospheric range, as well as general regional ranges identified by Gregoricka et al. (2020). (a) Local biospheric range. (b) Mediterranean Coast. (c) Eastern highlands. (d) Jordan Rift Valley. (e) Eastern corridor. (f) Western highlands [Colour figure can be viewed at [wileyonlinelibrary.com](https://onlinelibrary.wiley.com)]

region. Alakkam (2002) analyzed $\delta^{18}\text{O}$ in MB-LBA individuals from Ya'amun (sometimes spelled Ya'amoun) but did not investigate locality. Khirbet edh-Dharih in western Jordan during the Nabatean and Roman periods (ca. 1–300 CE) also experienced low levels of migration as identified using isotopic analysis (1/12, or 8%) (Perry et al., 2008). The assemblage from Byzantine Barsinia, also in northern Jordan like Pella, experienced no migration (0/12, 0%) (Al-Shorman & El-Khouri, 2011). Only one individual of the 31 analyzed (3%) in the Byzantine mining camp of Faynan in southwestern Jordan was suggested to be non-local (Perry et al., 2009). This is in contrast to another Byzantine site, Mount Nebo in western Jordan, which had a high percentage of non-locals (7/15, 47%) (Judd et al., 2019). There is no strong cultural reasoning to imagine that foreigners were drawn to Pella in the same way as to the Christian pilgrimage site of Mount Nebo, where people from across the Christian world might join monastic communities to gain grace in this life and beyond. Two Byzantine cemeteries of the Red Sea port of Aila show a hub of maritime connectivity during this time period, with 18 out of 22 individuals (82%) displaying non-local $^{87}\text{Sr}/^{86}\text{Sr}$ values (Perry et al., 2017). These later populations might not be appropriate comparison to Bronze Age Pella but highlight the breadth of experiences regarding migration and mobility in Jordan. With isotopic analyses finding populations containing between 0% and 82% non-locals in Jordan, there is clearly a range of experiences regarding first-generation immigration in Jordanian settlements over time and space.

The only other Jordanian Bronze Age mobility analysis using isotopes to date, Gregoricka et al. (2020) found seven out of 31 individuals (23%) interred in Bab adh-Dhra' in southern Jordan were likely non-locals. Comparison between Bab adh-Dhra' and Pella is fraught as Bab adh-Dhra' dates to the EBA, approximately 1,500 years earlier than the Pella MBA individuals, and located in a more marginal

environmental profile on the arid edge of the Dead Sea. Gregoricka et al. (2020) pointed out that the charnel houses they examined were not family tombs, but rather those of extended lineages, perhaps culturally curated (i.e., you could “become” a local on burial), thus accounting for the in-migration of people into this early settlement node.

If Bab adh-Dhra' is in a more marginal environment but contains a higher proportion of non-locals compared to Pella (23% compared to 14%), what does this say for Pella's connection to the rest of the ancient Near East and Mediterranean? The EBA is thought to have entailed the rise of urban centers followed by scattered autonomous settlements in Jordan (Harrison, 1997). Whether due to invasion/migration, rapid climate change, economic pressures, or other social and environmental changes, the transition from EBA-MBA is estimated to be marked by increasing sedentism and smaller spheres of interaction (Langgut et al., 2016; Miroshedji, 2009). The difference in immigration between Bab adh-Dhra' and Pella seems to mirror that cultural shift across the wider region. Artefactual evidence suggests that Pella as an MBA community had an active part in the wider economic and cultural network, but there are fewer non-locals buried in Pella's tombs than the marginal tombs of EBA Bab adh-Dhra'. Perhaps, this contrast between objects and people highlights Pella as a hub where traders moved goods along the wider Jordanian network, but immigrants were not largely drawn to settle at Pella.

The $\delta^{13}\text{C}$ values show a restricted range of less than 2‰ within the assemblage, suggesting that the population relied heavily on C_3 -based diet. This makes sense within the expected Bronze Age diet heavily reliant on C_3 cereals, legumes, and orchard crops for bread, vegetable accompaniment, and fodder for domesticated animals (Cartwright, 2003; Dickin et al., 2012; Fall et al., 1998, 2019; Sasson, 2016). When compared to other Jordanian sites, the Pella

individuals show more restricted $\delta^{13}\text{C}$ range than other groups with no outliers (Figure 8). The other three sites, in contrast, show wider range of values and more outliers in the groups.

Some of the higher $\delta^{13}\text{C}$ values at Mount Nebo were postulated to be partially a result of C_4 food intake (Judd et al., 2019). The wider ranges of values across these populations might also be a result of a variety of environments being utilized for C_3 input, especially in non-locals who came from other locations. With Pella showing less non-locals than Mount Nebo and Bab adh-Dhra', environmental variation in carbon stable isotope values might account for the wider range of values seen in more cosmopolitan settlements. Alternatively, these settlements with more non-locals might have had more immigrants practicing different foodway systems from those born in the region, recreating their homeland's cuisine in their new home and resisting dietary acculturation.

Regarding dental nonmetric data, the individuals represented by the teeth selected for isotopes analysis of Tomb 62 demonstrated wide morphological dispersal. Furthermore, the two individuals from tombs 106 and XXVIII share a closer morphological similarity (based on PAM clusters) with only 18% of the T.62 individuals sampled. The wide morphological dispersal of the Tomb 62 individuals suggests that they may not represent closely related individuals. There are two possible explanations. Tomb 62 may have been a cache of burials cleared from other tombs to make space, as suggested by Smith and Potts (1992), and the diversity seen in the tomb is a result of micro-evolution taking place at the site over a long period of time. Alternatively, the group(s) buried in Tomb 62 had a diverse ancestral background and their group collective (represented by the singular burial location) rose from something other than biological closeness. Prior analysis of a larger Pella assemblage using grouped data rather than individuals indicated strong shared affinity to the approximately contemporary site of Avaris in Northern Egypt (Maaranen, 2020). It is

unclear whether this similarity is due to regional closeness, as geographically closer sites tend to exhibit higher similarity (Irish, 2010; Zakrzewski, 2007), or indicates a more direct connection between the sites.

One of the four isotopic outliers was not available for biodistance analysis due to occlusal wear, but the other three are noted on Figure 6, individuals with Laboratory IDS 1042, 1047, and 1049. Again, all of these are from Tomb 62. Although identified as likely non-locals using isotopic analysis, none of them show isotopic values suggestive of the same homeland: 1042 has the highest $^{87}\text{Sr}/^{86}\text{Sr}$ ratio in the assemblage, and 1047's relatively low $^{87}\text{Sr}/^{86}\text{Sr}$ ratios denote this individual as an outlier, while 1049 displays $^{87}\text{Sr}/^{86}\text{Sr}$ ratios within the local range but has the highest $\delta^{18}\text{O}$ value in the assemblage. The small sample size prevents tests of statistical significance, and our observed differences between individuals are limited to five dental traits. Though a hindrance, this does not make all analyses impossible, evidenced by a recent publication where similarly few dental traits were useful when investigating the provenance of an individual buried in a Roman catacomb (Salesse et al., 2021). When combined with other lines of research and contextual information, even a qualitative interpretation such as the one presented here can be considered justified when keeping in mind the limitations.

7.2 | Conclusion

Significant movements of populations throughout the Middle Bronze Age are evidenced through funerary rituals and architecture (Andreou, 2016; Cohen, 2009; Ilan, 1995). These processes of relocation and re-integration constantly redefined peoples, groups, and sociocultural values. The findings of this bioarcheological study, together with the material evidence from Pella exhibiting relations

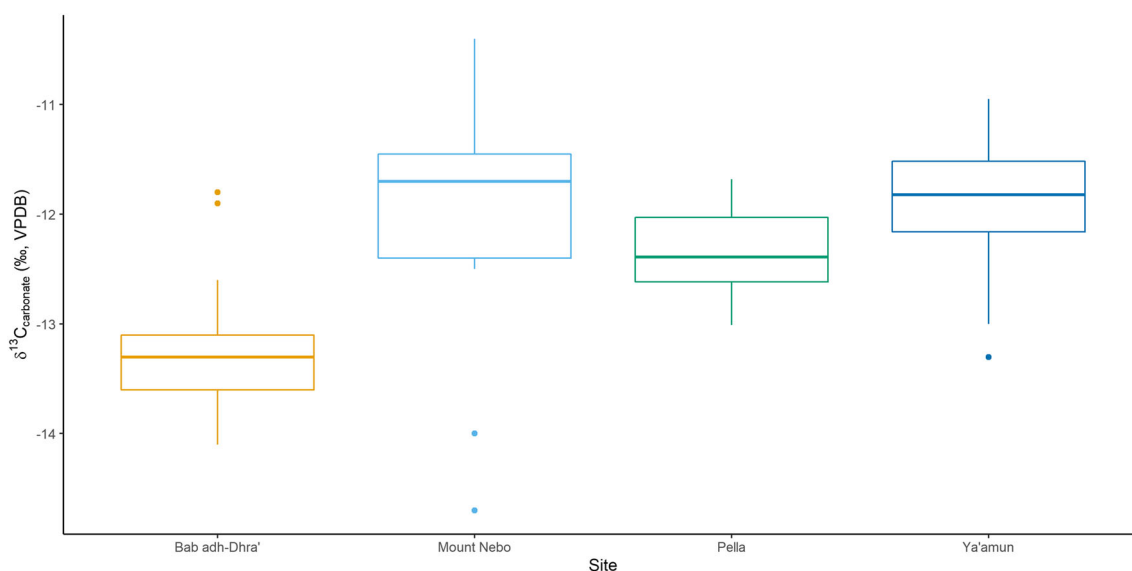


FIGURE 8 Boxplot of $\delta^{13}\text{C}$ Carbonate values of Pella and other Jordanian sites. Comparative data from Al-Shorman (2004), Gregoricka et al. (2020), and Judd et al. (2019) [Colour figure can be viewed at [wileyonlinelibrary.com](https://onlinelibrary.com)]

from Anatolia to Egypt, suggests the site was not as peripheral as its geographical location may have implied but rather was reached by a diverse assemblage of both artifacts and people alike, throughout the time period (the MBA) under study.

Expansion of the Jordanian biospheric information will help isotopic mobility studies postulate as to the origins of the non-locals identified isotopically within the wider region, although identifying the origin of non-locals will continue to be challenging due to issues of equifinality. Biodistance information has been lost due to material limitations in the assemblage, but the available dental traits suggest diverse ancestral background for the occupants of Tomb 62. Future research statistically integrating the two types of data are warranted, especially in sites where preservation is better and making use of the entirety of the ASUDAS traits, feasible in non-commingled burials.

ACKNOWLEDGMENTS

Thanks to Dr. Sam Rennie for sitting down for a whole Powerpoint on Zoom when all conferences were canceled, just so the first author could talk through the results with an “audience.” Joanne Peterkin was invaluable in helping prepare the carbonate samples. Funding to carry out this research was provided by the European Research Council (ERC) under the European Union's Horizon 2020 research and innovation program (H2020 European Research Council, grant agreement No 668640).

CONFLICT OF INTEREST

The authors have no conflict of interest to declare.

DATA AVAILABILITY STATEMENT

The data that support the findings of this study are available in the supporting information of this article as well as tables in-text.

ORCID

Chris Stantis  <https://orcid.org/0000-0001-7645-0233>

Nina Maaranen  <https://orcid.org/0000-0001-5821-1167>

Arwa Kharobi  <https://orcid.org/0000-0002-5642-3526>

Geoff M. Nowell  <https://orcid.org/0000-0003-3229-128X>

Colin Macpherson  <https://orcid.org/0000-0001-5302-6405>

Holger Schutkowski  <https://orcid.org/0000-0001-9527-4618>

REFERENCES

- Alakkam AA. 2002. Climate change and archaeological site distribution during the past four millennia in northern Jordan utilizing oxygen isotope analysis of human tooth enamel and geographic information system.
- Al-Bashaireh, K., Al-Shorman, A., Rose, J., Jull, A. T., & Hodgins, G. (2010). Paleodiet reconstruction of human remains from the archaeological site of Natfieh, northern Jordan. *Radiocarbon*, 52(2), 645–652. <https://doi.org/10.1017/S0033822200045677>
- Alexanderson V. 1978. Sukas V. A study of teeth and jaws from a Middle Bronze Age collective grave on tall Sukas.
- Al-Shorman, A. (2004). Stable carbon isotope analysis of human tooth enamel from the bronze age cemetery of Ya'amoun in Northern Jordan. *Journal of Archaeological Science*, 31(12), 1693–1698.
- Al-Shorman, A., & El-Khoury, L. (2011). Strontium isotope analysis of human tooth enamel from Barsinia: A late antiquity site in Northern Jordan. *Archaeological and Anthropological Sciences*, 3(3), 263–269. <https://doi.org/10.1007/s12520-011-0065-0>
- Alt, K. W., & Vach, W. (1995). Odontologic kinship analysis in skeletal remains: Concepts, methods, and results. *Forensic Science International*, 74(1–2), 99–113. [https://doi.org/10.1016/0379-0738\(95\)01740-A](https://doi.org/10.1016/0379-0738(95)01740-A)
- Andreou, P. (2016). Acting funerary ritual in variables. Preliminary thoughts on data structure and equivalence for comparative studies of funerary ritual in the Levant during the Middle Bronze Age. *Paléorient*, 42(2), 185–201. <https://doi.org/10.3406/paleo.2016.5726>
- Bender F. 1975. Geology of the Arabian peninsula. Geol Surv Prof Paper 560.
- Bentley GR. 1987. Kinship and social structure at Early Bronze IA Bab edh-Dhra', Jordan: A bioarchaeological analysis of the mortuary and dental data [PhD]: The University of Chicago.
- Bentley, R. A., Krause, R., Price, T. D., & Kaufmann, B. (2003). Human mobility at the early neolithic settlement of Vaihingen, Germany: Evidence from strontium isotope analysis. *Archaeometry*, 45(3), 471–486. <https://doi.org/10.1111/1475-4754.00122>
- Bentley, R. A., Price, T. D., & Stephan, E. (2004). Determining the ‘local’ ⁸⁷Sr/⁸⁶Sr range for archaeological skeletons: A case study from Neolithic Europe. *Journal of Archaeological Science*, 31(4), 365–375.
- Bentley, R. A., Buckley, H. R., Spriggs, M., Bedford, S., Ottley, C. J., Nowell, G. M., Macpherson, C. G., & Pearson, D. G. (2007). Lapita migrants in the Pacific's Oldest Cemetery: Isotopic analysis at Teouma, Vanuatu. *American Antiquity*, 72(4), 645–656.
- Bietak, M. (1997). The center of Hyksos rule: Avaris (Tell el-Daba). In E. D. Oren (Ed.), *The Hyksos: New historical and archaeological perspectives*. University Museum Symposium Series.
- Bourke, S. (2018). MBA Pella in Jordan: Intramural Graves and Extramural Cemeteries. In K. Kopetzky (Ed.), *Workshop 8: MBA tombs and their funerary environment*. XI ICAANE.
- Bourke, S., & Eriksson, K. (2006). Pella in Jordan, royal name scarabs and the Hyksos empire: a view from the margins. In E. Czerny, I. Hein, H. Hunger, D. Melman, & A. Schwab (Eds.), *Timelines studies in honour of Manfred Bietak* (pp. 339–348). Peeters.
- Bourke, S., Sparks, R., Schroeder, M., & Fischer, P. (2006). Pella in the Middle Bronze Age. In P. Fischer (Ed.), *The chronology of the Jordan Valley during the middle and late bronze ages: Pella, tell Abu al-Kharaz and tell Deir 'Alla* (pp. 9–58). Austrian Academy of Sciences.
- Bourke, S., Sparks, R., Sowada, K., & Mairs, L. (1994). Preliminary report on the University of Sydney's fourteenth season of excavations at Pella (Tabaqat Fahl) in 1992. *Annual of the Department of Antiquities of Jordan*, 38, 81–126.
- Bourke, S. J., & Sparks, R. T. (1995). The DAJ excavations at Pella in Jordan in 1963/64. In S. J. Bourke & J. P. Descoeudres (Eds.), *Trade, contact and the movement of peoples in the Eastern Mediterranean, studies in honour of Basil Hennessy* (pp. 149–167). Mediterranean Archaeology.
- Bowen GJ. 2018. The online isotopes in precipitation calculator, version OIPC2.2: University of Utah.
- Bowen GJ, West JB, Miller CC, Zhao L, and Zhang T. 2013. *IsoMAP: Isoscapes modeling, analysis and prediction* (version 1.0).
- Bryant, J. D., & Froelich, P. N. (1995). A model of oxygen isotope fractionation in body water of large mammals. *Geochimica et Cosmochimica Acta*, 59(21), 4523–4537. [https://doi.org/10.1016/0016-7037\(95\)00250-4](https://doi.org/10.1016/0016-7037(95)00250-4)
- Budd, P., Montgomery, J., Barreiro, B., & Thomas, R. G. (2000). Differential diagenesis of strontium in archaeological human dental tissues. *Applied Geochemistry*, 15(5), 687–694. [https://doi.org/10.1016/S0883-2927\(99\)00069-4](https://doi.org/10.1016/S0883-2927(99)00069-4)
- Cartwright, C. R. (2003). Grapes or raisins? An early Bronze Age larder under the microscope. *Antiquity*, 77(296), 345–348. <https://doi.org/10.1017/S0003598X00092322>

- Cavazzuti, C., Skeates, R., Millard, A. R., Nowell, G., Peterkin, J., Bernabò Brea, M., Cardarelli, A., & Salzani, L. (2019). Flows of people in villages and large centres in Bronze Age Italy through strontium and oxygen isotopes. *PLoS ONE*, 14(1), e0209693. <https://doi.org/10.1371/journal.pone.0209693>
- Chai, H., Lee, J. J.-W., Constantino, P. J., Lucas, P. W., & Lawn, B. R. (2009). Remarkable resilience of teeth. *Proceedings of the National Academy of Sciences*, 106(18), 7289–7293. <https://doi.org/10.1073/pnas.0902466106>
- Chenery, C. A., Müldner, G., Evans, J., Eckardt, H., & Lewis, M. (2010). Strontium and stable isotope evidence for diet and mobility in Roman Gloucester, UK. *Journal of Archaeological Science*, 37(1), 150–163.
- Chenery, C. A., Pashley, V., Lamb, A. L., Sloane, H. J., & Evans, J. A. (2012). The oxygen isotope relationship between the phosphate and structural carbonate fractions of human bioapatite. *Rapid Communications in Mass Spectrometry*, 26(3), 309–319. <https://doi.org/10.1002/rcm.5331>
- Clamer, C. (1977). A burial cave near Nablus (Tell Balata). *IEJ*, 27(1), 48.
- Cohen, S. L. (2009). Continuities and discontinuities: A reexamination of the intermediate bronze age–Middle bronze age transition in Canaan. *Bulletin of the American Schools of Oriental Research*, 354(1), 1–13. <https://doi.org/10.1086/BASOR25609312>
- Cohen, S. L. (2018). *Canaanites, chronologies, and connections: The relationship of Middle Bronze IIA Canaan to Middle Kingdom Egypt*. Brill.
- Cooley, R. E., & Pratico, G. D. (1994). Tell Dothan: The western cemetery, with comments on Joseph Free's excavations, 1953 to 1964. In W. G. Dever (Ed.), *Preliminary excavation report: Sardis, Bir umm Fawakhir, tell el-'Umeiri, the combined Caesarea expeditions, and tell Dothan* (pp. 147–190). The American Schools of Oriental Research.
- Daux, V., Lécuyer, C., Héran, M.-A., Amiot, R., Simon, L., Fourel, F., Martineau, F., Lynnerup, N., Reyckler, H., & Escarguel, G. (2008). Oxygen isotope fractionation between human phosphate and water revisited. *Journal of Human Evolution*, 55(6), 1138–1147. <https://doi.org/10.1016/j.jhevol.2008.06.006>
- de Haas, H., & Rodríguez, F. (2010). Mobility and human development: Introduction. *Journal of Human Development and Capabilities*, 11(2), 177–184. <https://doi.org/10.1080/19452821003696798>
- Delgado, M., Ramírez, L. M., Adhikari, K., Fuentes-Guajardo, M., Zanolli, C., Gonzalez-José, R., Canizales, S., Bortolini, M. C., Poletti, G., & Gallo, C. (2019). Variation in dental morphology and inference of continental ancestry in admixed Latin Americans. *American Journal of Physical Anthropology*, 168(3), 438–447. <https://doi.org/10.1002/ajpa.23756>
- DeNiro, M. J., & Epstein, S. (1978). Influence of diet on the distribution of carbon isotopes in animals. *Geochimica et Cosmochimica Acta*, 42(5), 495–506. [https://doi.org/10.1016/0016-7037\(78\)90199-0](https://doi.org/10.1016/0016-7037(78)90199-0)
- Dicke-Toupin CR. 2012. Population continuity or replacement at ancient Lachish? A dental affinity analysis in the Levant.
- Dickin, E., Steele, K., Edwards-Jones, G., & Wright, D. (2012). Agronomic diversity of naked barley (*Hordeum vulgare* L.): A potential resource for breeding new food barley for Europe. *Euphytica*, 184(1), 85–99. <https://doi.org/10.1007/s10681-011-0567-y>
- Edwards PC. 2013. The Pella region: Environment and resources in the terminal Pleistocene. Wadi Hammeh 27, an early Natufian settlement at Pella in Jordan: BRILL. 17–33.
- Elias N. 2016. Pratiques funéraires et identités biologiques à Berytus et à Botrys à l'époque romaine (Liban, Ier siècle av. J.-C.-IVème siècle apr. J.-C.) [PhD]: Université de Bordeaux.
- Fall, P. L., Falconer, S. E., & Porson, S. (2019). Archaeobotanical inference of intermittent settlement and agriculture at Middle Bronze Age Zahrat adh-Dhra'1, Jordan. *Journal of Archaeological Science: Reports*, 26, 101884. <https://doi.org/10.1016/j.jasrep.2019.101884>
- Fall, P. L., Lines, L., & Falconer, S. E. (1998). Seeds of civilization: Bronze age rural economy and ecology in the southern Levant. *Annals of the Association of American Geographers*, 88(1), 107–125. <https://doi.org/10.1111/1467-8306.00087>
- France, C. A. M., Sugiyama, N., & Aguayo, E. (2020). Establishing a preservation index for bone, dentin, and enamel bioapatite mineral using ATR-FTIR. *Journal of Archaeological Science: Reports*, 33, 102551.
- Gregoricka, L. A., Ullinger, J., & Sheridan, S. G. (2020). Status, kinship, and place of burial at Early Bronze Age Bab adh-Dhra': A biogeochemical comparison of charnel house human remains. *American Journal of Physical Anthropology*, 171(2), 319–335. <https://doi.org/10.1002/ajpa.23982>
- Grimmeisen, F., Lehmann, M. F., Liesch, T., Goepfert, N., Klinger, J., Zopfi, J., & Goldscheider, N. (2017). Isotopic constraints on water source mixing, network leakage and contamination in an urban groundwater system. *Science of the Total Environment*, 583, 202–213. <https://doi.org/10.1016/j.scitotenv.2017.01.054>
- Haber, M., Doumet-Serhal, C., Scheib, C., Xue, Y., Danecek, P., Mezzavilla, M., Youhanna, S., Martiniano, R., Prado-Martinez, J., Szpak, M., Matisoo-Smith, E., Schutkowski, H., Mikulski, R., Zalloua, P., Kivisild, T., & Tyler-Smith, C. (2017). Continuity and admixture in the last five millennia of Levantine history from ancient Canaanite and present-day Lebanese genome sequences. *The American Journal of Human Genetics*, 101(2), 274–282. <https://doi.org/10.1016/j.ajhg.2017.06.013>
- Harrison, T. P. (1997). Shifting patterns of settlement in the highlands of Central Jordan during the Early Bronze Age. *Bulletin of the American Schools of Oriental Research*, 306(1), 1–37. <https://doi.org/10.2307/1357546>
- Hartman, G., & Danin, A. (2010). Isotopic values of plants in relation to water availability in the eastern Mediterranean region. *Oecologia*, 162(4), 837–852. <https://doi.org/10.1007/s00442-009-1514-7>
- Hartman, G., & Richards, M. (2014). Mapping and defining sources of variability in bioavailable strontium isotope ratios in the Eastern Mediterranean. *Geochimica et Cosmochimica Acta*, 126(Supplement C), 250–264.
- Hefner, J. T., Pilloud, M. A., Buikstra, J., & Vogelsberg, C. (2016). A brief history of biological distance analysis. *Biological Distance Analysis*, 3–22. <https://doi.org/10.1016/B978-0-12-801966-5.00001-9>
- Henderson, J., Evans, J., & Barkoudah, Y. (2009). The roots of provenance: Glass, plants and isotopes in the Islamic Middle East. *Antiquity*, 83(320), 414–429. <https://doi.org/10.1017/S0003598X00098525>
- Hennessy, J. B., McNicoll, A., Potts, T., & Walmsley, A. (1981). Preliminary report on a second season of excavation at Pella, Jordan (winter, 1980). *Annual of the Department of Antiquities*, 25, 267–309.
- Hodell, D. A., Mead, G. A., & Mueller, P. A. (1990). Variation in the strontium isotopic composition of seawater (8 Ma to present): Implications for chemical weathering rates and dissolved fluxes to the oceans. *Chemical Geology: Isotope Geoscience Section*, 80(4), 291–307.
- Hoppe, K. A., Koch, P. L., & Furutani, T. T. (2003). Assessing the preservation of biogenic strontium in fossil bones and tooth enamel. *International Journal of Osteoarchaeology*, 13(1–2), 20–28. <https://doi.org/10.1002/oa.663>
- Hubbard, A. R., Guatelli-Steinberg, D., & Irish, J. D. (2015). Do nuclear DNA and dental nonmetric data produce similar reconstructions of regional population history? An example from modern coastal Kenya. *American Journal of Physical Anthropology*, 157(2), 295–304. <https://doi.org/10.1002/ajpa.22714>
- Ilan, D. (1995). The Dawn Of Internationalism- The Middle Bronze Age. In T. E. Levy (Ed.), *The archaeology of society in the Holy Land* (pp. 297–319). Leicester University Press.
- Irish, J. D. (2010). The mean measure of divergence: Its utility in model-free and model-bound analyses relative to the Mahalanobis D2 distance for nonmetric traits. *American Journal of Human Biology*, 22(3), 378–395. <https://doi.org/10.1002/ajhb.21010>
- Johnson, C. M., Lipman, P. W., & Czamanske, G. K. (1990). H, O, Sr, Nd, and Pb isotope geochemistry of the Latir volcanic field and cogenetic intrusions, New Mexico, and relations between evolution of a continental magmatic center and modifications of the lithosphere.

- Contributions to Mineralogy and Petrology*, 104(1), 99–124. <https://doi.org/10.1007/BF00310649>
- Judd, M., Gregoricka, L., & Foran, D. (2019). The monastic mosaic at Mount Nebo, Jordan: Biogeochemical and epigraphical evidence for diverse origins. *Antiquity*, 1–18.
- Kamenov, G. D., Lofaro, E. M., Goad, G., & Krigbaum, J. (2018). Trace elements in modern and archaeological human teeth: Implications for human metal exposure and enamel diagenetic changes. *Journal of Archaeological Science*, 99, 27–34.
- Knapp, A. B. (1993). *Society and polity at Bronze Age Pella: An Annales perspective*. Sheffield Academic Press.
- Langgut, D., Adams, M. J., & Finkelstein, I. (2016). Climate, settlement patterns and olive horticulture in the southern Levant during the Early Bronze and Intermediate Bronze Ages (c. 3600–1950 BC). *Levant*, 48(2), 117–134. <https://doi.org/10.1080/00758914.2016.1193323>
- Langgut, D., Finkelstein, I., & Litt, T. (2013). Climate and the Late Bronze collapse: New evidence from the southern Levant. *Tel Aviv*, 40(2), 149–175. <https://doi.org/10.1179/033443513X13753505864205>
- Lee-Thorp, J. A., Sealy, J. C., & van der Merwe, N. J. (1989). Stable carbon isotope ratio differences between bone collagen and bone apatite, and their relationship to diet. *Journal of Archaeological Science*, 16(6), 585–599.
- Lee-Thorp, J. A., & van der Merwe, N. J. (1991). Aspects of the chemistry of modern and fossil biological apatites. *Journal of Archaeological Science*, 18(3), 343–354.
- Lewis, J., Pike, A. W. G., Coath, C. D., & Evershed, R. P. (2017). Strontium concentration, radiogenic ($^{87}\text{Sr}/^{86}\text{Sr}$) and stable ($\delta^{88}\text{Sr}$) strontium isotope systematics in a controlled feeding study. *STAR: Science & Technology of Archaeological Research*, 3(1), 45–57. <https://doi.org/10.1080/20548923.2017.1303124>
- Lightfoot, E., & O'Connell, T. C. (2016). On the use of biomineral oxygen isotope data to identify human migrants in the archaeological record: Intra-sample variation, statistical methods and geographical considerations. *PLoS ONE*, 11(4), e0153850. <https://doi.org/10.1371/journal.pone.0153850>
- Longinelli, A. (1984). Oxygen isotopes in mammal bone phosphate: A new tool for paleohydrological and paleoclimatological research? *Geochimica et Cosmochimica Acta*, 48(2), 385–390. [https://doi.org/10.1016/0016-7037\(84\)90259-X](https://doi.org/10.1016/0016-7037(84)90259-X)
- Lovell, N. C., & Scott Haddow, S. (2006). Nonmetric analysis of the permanent dentition of bronze age tell Leilan, Syria. *International Journal of Dental Anthropology*, 9, 1–7.
- Lucke, B., Ziadat, F., & Taimeh, A. (2014). *The soils of Jordan*. Presses de l'Institut Français du Proche-Orient. <https://doi.org/10.4000/books.ifpo.4867>
- Maaranen, N. (2020). *Ties that bind: Investigating Hyksos provenance and migration using dental morphology*. Bournemouth University.
- Maaranen, N., Zakrzewski, S., & Schutkowski, H. (2019). Hyksos in Egypt—utilising biodistance methods to interpret archaeological and textual evidence from Tell el-Dab'a. *American Journal of Physical Anthropology*, 168, 149–149.
- Maechler M, Rousseeuw P, Struyf A, Hubert M, and Hornik K. 2019. Cluster: Cluster analysis basics and extensions. R package version 2.1.0.
- Marado, L. M., & Silva, A. M. (2016). The mandibular molar pit-tubercle (MMPT) dental nonmetric trait: Comprehensive analysis of a large sample. *Homo*, 67(6), 462–470. <https://doi.org/10.1016/j.jchb.2016.09.003>
- McNicoll, A., Edwards, P., Hanbury-Tenison, J., Hennessy, B., Potts, T., Smith, R., Walmsley, A., & Watson, P. (1992). *Pella in Jordan 2 Sydney*. Meditarch.
- McNicoll, A., Smith, R. H., & Hennessy, B. (1982). *Pella in Jordan 1*. Australian National Gallery.
- Miroschedji, P. (2009). *Rise and collapse in the Southern Levant in the Early Bronze Age*. Edizioni Quasar.
- Moorrees, C. F. A., Fanning, E. A., & Hunt, E. E. (1963). Age variation of formation stages for ten permanent teeth. *Journal of Dental Research*, 42(6), 1490–1502. <https://doi.org/10.1177/00220345630420062701>
- Nassar, J. (2010). *Les espaces funéraires infra-urbains de Mari (Moyen-Euphrate, 2900–1760 AV.J.-C.), analyse archéo-anthropologique [PhD]*. University of Bordeaux.
- North, R. (1965). *The excavations of Dominus Flevit (Vol. 2)*. JSTOR.
- Obeidat, M., Awawdeh, M., Matiatos, I., Al-Ajlouni, A., & Al-Mughaid, H. (2021). Identification and apportionment of nitrate sources in the phreatic aquifers in northern Jordan using a dual isotope method ($\delta^{15}\text{N}$ and $\delta^{18}\text{O}$ of NO_3^-). *Groundwater for Sustainable Development*, 12, 100505. <https://doi.org/10.1016/j.gsd.2020.100505>
- Özbek M. 1975. *Hombres de Byblos: étude comparative des squelettes des âges des métaux au Proche-Orient: éditeur non identifié*.
- Pacheco-Forés, S. I., Morehart, C. T., Buikstra, J. E., Gordon, G. W., & Knudson, K. J. (2021). Migration, violence, and the “other”: A biogeochemical approach to identity-based violence in the Epiclassic Basin of Mexico. *Journal of Anthropological Archaeology*, 61, 101263.
- Parras Z. 2004. *The biological affinities of the eastern Mediterranean in the chalcolithic and bronze age: A regional dental non-metric approach: University of Sheffield, DOI: https://doi.org/10.30861/9781841713823*
- Pederzani, S., & Britton, K. (2018). Oxygen isotopes in bioarchaeology: Principles and applications, challenges and opportunities. *Earth-Science Reviews*, 188, 77–107. <https://doi.org/10.1016/j.earscirev.2018.11.005>
- Perry, M. A., Coleman, D., & Delhopital, N. (2008). Mobility and exile at 2nd century A.D. Khirbet edh-Dharih: Strontium isotope analysis of human migration in western Jordan. *Geoarchaeology*, 23(4), 528–549. <https://doi.org/10.1002/gea.20230>
- Perry, M. A., Coleman, D. S., Dettman, D. L., & al-Shiyab AH. (2009). An isotopic perspective on the transport of byzantine mining camp laborers into southwestern Jordan. *American Journal of Physical Anthropology*, 140(3), 429–441. <https://doi.org/10.1002/ajpa.21085>
- Perry, M. A., Coleman, D. S., Dettman, D. L., Grattan, J. P., & Halim al-Shiyab, A. H. (2011). Condemned to metallum? The origin and role of 4th–6th century A.D. Phaeno mining camp residents using multiple chemical techniques. *Journal of Archaeological Science*, 38(3), 558–569.
- Perry, M. A., Jennings, C., & Coleman, D. S. (2017). Strontium isotope evidence for long-distance immigration into the Byzantine port city of Aila, modern Aqaba, Jordan. *Archaeological and Anthropological Sciences*, 9(5), 943–964. <https://doi.org/10.1007/s12520-016-0314-3>
- Potts, T. F., Colledge, S. M., & Edwards, P. C. (1985). Preliminary report on a sixth season of excavation by the University of Sydney at Pella in Jordan (1983/84). *Annual of the Department of Antiquities of Jordan*, 29, 181–210.
- Price, T. D., Burton, J. H., & Bentley, R. A. (2002). The characterization of biologically available strontium isotope ratios for the study of prehistoric migration. *Archaeometry*, 44(1), 117–135. <https://doi.org/10.1111/1475-4754.00047>
- Price, T. D., Burton, J. H., Fullagar, P. D., Wright, L. E., Buikstra, J. E., & Tiesler, V. (2008). Strontium isotopes and the study of human mobility in ancient Mesoamerica. *Latin American Antiquity*, 19(2), 167–180. <https://doi.org/10.1017/S1045663500007781>
- Prowse, T. L., Schwarcz, H. P., Garnsey, P., Knyf, M., Macchiarelli, R., & Bondioli, L. (2007). Isotopic evidence for age-related immigration to imperial Rome. *American Journal of Physical Anthropology*, 132(4), 510–519. <https://doi.org/10.1002/ajpa.20541>
- R Core Team. 2000. R language definition. Vienna, Austria: R foundation for statistical computing.
- Recht L. 2018. *Human sacrifice: Archaeological perspectives from around the world: Cambridge University press, DOI: https://doi.org/10.1017/9781108610322*

- Ricaut, F. X., Auriol, V., von Cramon-Taubadel, N., Keyser, C., Murail, P., Ludes, B., & Crubézy, E. (2010). Comparison between morphological and genetic data to estimate biological relationship: The case of the Egin Gol necropolis (Mongolia). *American Journal of Physical Anthropology*, 143(3), 355–364. <https://doi.org/10.1002/ajpa.21322>
- Rousseeuw, P. J., Ruts, I., & Tukey, J. W. (1999). The bagplot: A bivariate boxplot. *The American Statistician*, 53(4), 382–387.
- Rozzi, F. R. (2016). Diversity in tooth eruption and life history in humans: Illustration from a pygmy population. *Scientific Reports*, 6(1), 1–10.
- Sage, R. F., & Monson, R. K. (1998). *C₄ plant biology*. Academic Press.
- Salesse, K., Dufour, É., Balter, V., Tykot, R. H., Maaranen, N., Rivollat, M., Kharobi, A., Deguilloux, M.-F., Pemonge, M.-H., & Brůžek, J. (2021). Far from home: A multi-analytical approach revealing the journey of an African-born individual to imperial Rome. *Journal of Archaeological Science: Reports*, 37, 103011. <https://doi.org/10.1016/j.jasrep.2021.103011>
- Salesse, K., Fernandes, R., de Rochefort, X., Brůžek, J., Castex, D., & Dufour, É. (2018). IsoArch.Eu: An open-access and collaborative isotope database for bioarchaeological samples from the Graeco-Roman world and its margins. *Journal of Archaeological Science: Reports*, 19(June), 1050–1055. <https://doi.org/10.1016/j.jasrep.2017.07.030>
- Sasson, A. (2016). *Animal husbandry in ancient Israel: A zooarchaeological perspective on livestock exploitation, herd management and economic strategies*. Routledge. <https://doi.org/10.4324/9781315541259>
- Scott, G., & Irish, J. (2017). *Human tooth crown and root morphology: The Arizona State University dental anthropology system*. Cambridge University Press. <https://doi.org/10.1017/9781316156629>
- Scott, G. R., Pilloud, M., Navega, D., Coelho, J., Cunha, E., & Irish, J. (2018). rASUDAS: A new web-based application for estimating ancestry from tooth morphology. *Forensic Anthropology*, 1(1), 18–31. <https://doi.org/10.5744/fa.2018.0003>
- Scott, G. R., & Turner, C. G. II (1997). *The anthropology of modern human teeth: Dental morphology and its variation in recent human populations*. Cambridge University Press. <https://doi.org/10.1017/CBO9781316529843>
- Scott, G. R., Turner, C. G. II, Townsend, G. C., & Martínón-Torres, M. (2018). *The anthropology of modern human teeth*. Cambridge University Press. <https://doi.org/10.1017/9781316795859>
- Seger, J., and Lance D. 1988. Gezer V. Jerusalem: Annual of the Hebrew Union College Nelson Glueck School of Biblical Archaeology.
- Sharp ZD. 2017. Principles of stable isotope geochemistry, Second Edition. Published Online.
- Shaw, J. E., Baker, J. A., Menzies, M. A., Thirlwall, M., & Ibrahim, K. (2003). Petrogenesis of the largest intraplate volcanic field on the Arabian plate (Jordan): A mixed lithosphere-asthenosphere source activated by lithospheric extension. *Journal of Petrology*, 44.
- Sheridan, S. G., & Gregoricka, L. A. (2015). Monks on the move: Evaluating pilgrimage to byzantine St. Stephen's monastery using strontium isotopes. *American Journal of Physical Anthropology*, 158(4), 581–591. <https://doi.org/10.1002/ajpa.22827>
- Shewan, L. (2004). Natufian settlement systems and adaptive Strategies: The issue of sedentism and the potential of strontium isotope analysis. In C. Delage (Ed.), *The last hunter-gatherers in the near east* (pp. 55–94). Oxford, UK.
- Shoko, C., Mutanga, O., & Dube, T. (2016). Progress in the remote sensing of C₃ and C₄ grass species aboveground biomass over time and space. *ISPRS Journal of Photogrammetry and Remote Sensing*, 120, 13–24. <https://doi.org/10.1016/j.isprsjprs.2016.08.001>
- Smith, B. H. (1984). Patterns of molar wear in hunter-gatherers and agriculturalists. *American Journal of Physical Anthropology*, 63(1), 39–56. <https://doi.org/10.1002/ajpa.1330630107>
- Smith, R. H. (1973). *Pella of the Decapolis I: The 1967 season of the College of Wooster Expedition to Pella*. College of Wooster.
- Smith, R. H., & Potts, T. (1992). The Middle and Late Bronze Ages. In A. McNicoll (Ed.), *Pella in Jordan 2: The second interim report of the joint University of Sydney and the College of Wooster excavations at Pella, 1982–1985* (pp. 35–81). Meditarch.
- Smits, E., Millard, A. R., Nowell, G., & Pearson, D. G. (2010). Isotopic investigation of diet and residential mobility in the Neolithic of the lower Rhine Basin. *European Journal of Anaesthesiology*, 13(1), 5–31. <https://doi.org/10.1177/1461957109355040>
- Sołtysiak, A. (2019). Strontium and nitrogen isotopic evidence of food import to tell Ashara–Terqa, a Bronze Age city on the Euphrates, Syria. *International Journal of Osteoarchaeology*, 29(1), 127–133. <https://doi.org/10.1002/oa.2724>
- Sołtysiak, A., & Bialon, M. (2013). Population history of the middle Euphrates valley: Dental non-metric traits at Tell Ashara, Tell Masaikh and Jebel Mashtale, Syria. *Homo*, 64(5), 341–356. <https://doi.org/10.1016/j.jchb.2013.04.005>
- Stager, L. E. (2001). Port power in the early and middle bronze age: The organisation of hinterland trade and production. In S. Wolff (Ed.), *Studies in the archaeology of Israel and Neighbouring lands in memory of Douglas L Esse Winona Lake* (pp. 625–638). Eisenbrauns.
- Stantis, C., Buckley, H. R., Kinaston, R. L., Nunn, P. D., Jaouen, K., & Richards, M. P. (2016). Isotopic evidence of human mobility and diet in a prehistoric/protohistoric Fijian coastal environment (c. 750–150 BP). *American Journal of Physical Anthropology*, 159(3), 478–495. <https://doi.org/10.1002/ajpa.22884>
- Stantis, C., Kharobi, A., Maaranen, N., Nowell, G. M., Bietak, M., Prell, S., & Schutkowski, H. (2020). Who were the Hyksos? Challenging traditional narratives using strontium isotope (⁸⁷Sr/⁸⁶Sr) analysis of human remains from ancient Egypt. *PLoS ONE*, 15(7), e0235414. <https://doi.org/10.1371/journal.pone.0235414>
- Stantis, C., Kinaston, R. L., Richards, M. P., Davidson, J. M., & Buckley, H. R. (2015). Assessing human diet and movement in the Tongan maritime chiefdom using isotopic analyses. *PLoS ONE*, 10(3), e0123156. <https://doi.org/10.1371/journal.pone.0123156>
- Stantis, C., & Schutkowski, H. (2019). Stable Isotope Analyses to Investigate Hyksos Identity and Origins. In M. Bietak & S. Prell (Eds.), *The enigma of the Hyksos Wiesbaden* (pp. 321–338). Harrassowitz Verlag.
- Stark, R. J., Emery, M. V., Schwarcz, H., Sperduti, A., Bondioli, L., Craig, O. E., & Prowse, T. (2020). Imperial Roman mobility and migration at Velia (1st to 2nd c. CE) in southern Italy. *Journal of Archaeological Science*, 30, 102217.
- Stein, M., Starinsky, A., Katz, A., Goldstein, S. L., Machlus, M., & Schramm, A. (1997). Strontium isotopic, chemical, and sedimentological evidence for the evolution of Lake Lisan and the Dead Sea. *Geochimica et Cosmochimica Acta*, 61(18), 3975–3992. [https://doi.org/10.1016/S0016-7037\(97\)00191-9](https://doi.org/10.1016/S0016-7037(97)00191-9)
- Stojanowski, C., & Hubbard, A. (2017). Sensitivity of dental phenotypic data for the identification of biological relatives. *International Journal of Osteoarchaeology*, 27(5), 813–827. <https://doi.org/10.1002/oa.2596>
- Stojanowski, C. M., & Schillaci, M. A. (2006). Phenotypic approaches for understanding patterns of intracemetery biological variation. *American Journal of Physical Anthropology*, 131(S43), 49–88. <https://doi.org/10.1002/ajpa.20517>
- Terakado, Y., Shimizu, H., & Masuda, A. (1988). Nd and Sr isotopic variations in acidic rocks formed under a peculiar tectonic environment in Miocene Southwest Japan. *Contributions to Mineralogy and Petrology*, 99(1), 1–10. <https://doi.org/10.1007/BF00399360>
- Thesleff, I. (2006). The genetic basis of tooth development and dental defects. *American Journal of Medical Genetics. Part A*, 140(23), 2530–2535. <https://doi.org/10.1002/ajmg.a.31360>
- Thesleff, I. (2014). Current understanding of the process of tooth formation: Transfer from the laboratory to the clinic. *Australian Dental Journal*, 59(Suppl 1), 48–54. <https://doi.org/10.1111/adj.12102>
- Thomsen, E., & Andreassen, R. (2019). Agricultural lime disturbs natural strontium isotope variations: Implications for provenance and migration studies. *Science Advances*, 5(3), eaav8083.

- Torrence, R. (1986). *Production and exchange of stone tools: Prehistoric obsidian in the Aegean*. Cambridge University Press.
- Torrence, R., Specht, J., Fullagar, R., & Bird, R. (1992). From Pleistocene to present: Obsidian sources in West New Britain, Papua New Guinea. *Records of the Australian Museum, Supplement*, 15, 83–98. <https://doi.org/10.3853/j.0812-7387.15.1992.86>
- Townsend, G., Bockmann, M., Hughes, T., & Brook, A. (2012). Genetic, environmental and epigenetic influences on variation in human tooth number, size and shape. *Odontology*, 100(1), 1–9. <https://doi.org/10.1007/s10266-011-0052-z>
- Townsend, G., Harris, E. F., Lesot, H., Clauss, F., & Brook, A. (2009). Morphogenetic fields within the human dentition: A new, clinically relevant synthesis of an old concept. *Arch Oral Biol* 54 Suppl, 1(Suppl 1), S34–S44.
- Trickett, M. A., Budd, P., Montgomery, J., & Evans, J. (2003). An assessment of solubility profiling as a decontamination procedure for the $^{87}\text{Sr}/^{86}\text{Sr}$ analysis of archaeological human skeletal tissue. *Applied Geochemistry*, 18(5), 653–658. [https://doi.org/10.1016/S0883-2927\(02\)00181-6](https://doi.org/10.1016/S0883-2927(02)00181-6)
- Trueman, C. N., Privat, K., & Field, J. (2008). Why do crystallinity values fail to predict the extent of diagenetic alteration of bone mineral? Palaeogeography, Palaeoclimatology, Palaeoecology, 266(3), 160–167. <https://doi.org/10.1016/j.palaeo.2008.03.038>
- Ullinger, J. M., Sheridan, S. G., Hawkey, D. E., Turner, C. G., & Cooley, R. (2005). Bioarchaeological analysis of cultural transition in the southern Levant using dental nonmetric traits. *American Journal of Physical Anthropology*, 128(2), 466–476. <https://doi.org/10.1002/ajpa.20074>
- van der Maaten, L., & Hinton, G. (2008). Visualizing data using t-SNE. *Journal of Machine Learning Research*, (9), 2579–2605.
- Walmsley, A., Macumber, P., Edwards, P., Bourke, S., & Watson, P. (1993). The eleventh and twelfth seasons of excavations at Pella (Tabaqat Fah) 1989–1990. *Annual of the Department of Antiquities of Jordan*, 37, 165–240.
- Weets, J. (2009). A promising mandibular molar trait in ancient populations of Ireland. *Dental Anthropology*, (22), 65–72.
- Wolf HP, and Bielefeld U. 2019. aplpack: Another plot PACKage: Stem, leaf, bagplot, faces, spin3R, plotsummary, plothulls, and some slider functions. (version 190512).
- Yadin, Y., Aharoni, Y., Amiran, R., Dothan, T., Dunayevsky, I., & Perrot, J. (1960). *Hazor II: An account of the second season of excavations, 1956*. Magnes Press.
- Zakrzewski, S. R. (2007). Population continuity or population change: Formation of the ancient Egyptian state. *American Journal of Physical Anthropology*, 132(4), 501–509. <https://doi.org/10.1002/ajpa.20569>
- Zoubov, A. A. (2011). *Odontoglyphics: The laws of variation of the human molar crown microrelief*. De Gruyter Mouton.

SUPPORTING INFORMATION

Additional supporting information may be found in the online version of the article at the publisher's website.

How to cite this article: Stantis, C., Maaranen, N., Kharobi, A., Nowell, G. M., Macpherson, C., Schutkowski, H., & Bourke, S. (2021). Jordanian migration and mobility in the Middle Bronze Age (ca. 2100–1550 BCE) at Pella. *International Journal of Osteoarchaeology*, 1–19. <https://doi.org/10.1002/oa.3069>